Neuronal primary cilia regulate pyramidal cell positioning to the deep and superficial sublayers in the hippocampal CA1

Juan Yang[1], Liyan Qiu[1], and Xuanmao Chen[1, *]

[1] Department of Molecular, Cellular, and Biomedical Sciences, University of New Hampshire, Durham, NH 03824

[*] Correspondence should be addressed to Dr. Xuanmao Chen:

Department of Molecular, Cellular, and Biomedical Sciences, College of Life Sciences and Agriculture, University of New Hampshire,

389 Rudman Hall, 46 College Road, Durham, NH 03824. Phone: 603 862 4542, Fax: 603 862 4013, Email: Xuanmao.Chen@unh.edu

Running Title: Primary Cilia and Pyramidal Cell Positioning

Key Words: Neuronal Primary Cilia, Pyramidal Cell Positioning, Arl13B and AC3, Inside-Out Lamination, and Neuronal Maturation

Acknowledgements: This study was supported by National Institutes of Health Grants K01AG054729, P20GM113131-7006, R15MH126317, and R15MH125305 to X.C.; A UNH CoRE PRP award and Cole Neuroscience and Behavioral Faculty Research Awards to X.C.; UNH Summer TA Research Fellowships (STAF) to J.Y. We are grateful to the University Instrumentation Center at UNH for excellent A1R HD confocal imaging service. We thank the scientists who have helped to generate the Arl13B-mCherry; Centrin2-GFP double transgenic mouse model.

Abstract

It is well-recognized that primary cilia regulate embryonic neurodevelopment, but little is known about their roles in postnatal neurodevelopment. The striatum pyramidal (SP) of hippocampal CA1 consists of superficial and deep sublayers, however, it is not well understood how early- and late-born pyramidal neurons position to two sublayers postnatally. Here we show that neuronal primary cilia emerge after CA1 pyramidal cells have reached SP, but before final neuronal positioning. The axonemes of primary cilia of early-born neurons point to the stratum oriens (SO), whereas late-born neuronal cilia orient toward the stratum radiatum (SR), reflecting an inside-out lamination pattern. Neuronal primary cilia in SP undergo marked changes in morphology and orientation from postnatal day 5 (P5) to P14, concurrent with pyramidal cell positioning to the deep and superficial sublayers and with neuronal maturation. Transgenic overexpression of Arl13B, a protein regulating ciliogenesis, not only elongates primary cilia and promotes earlier cilia protrusion, but also affects centriole positioning and cilia orientation in SP. The centrioles of late-born neurons migrate excessively to cluster at SP bottom before primary cilia protrusion and a reverse movement back to the main SP. Similarly, this "pull-back" movement of centriole/cilia is also identified on late-born cortical pyramidal neurons, although early- and late-born cortical neurons display the same cilia orientation. Together, this study provides the first evidence demonstrating that late-born pyramidal neurons exhibit a reverse movement for cell positioning, and primary cilia regulate pyramidal neuronal positioning to the deep and superficial sublayers in the hippocampus.

Introduction

Neuronal primary cilia are hair-like, microtubule-based surface projections, which are identified throughout the nervous system including the hippocampus and cortex (1-3). Neuronal primary cilia are sensitive to diverse extracellular signals, such as hormones and neurotransmitters, and regulate a variety of physiological functions including neurodevelopment, energy balance, and cognitive function (3-6). Defects in neuronal primary cilia lead to various brain disorders including developmental disorders, obesity, and cognitive impairment (4, 6-11). It is well-known that primary cilia modulate embryonic neurodevelopment (12, 13) by mediating the Sonic hedgehog (Shh) signaling (3, 4, 6, 14, 15) and influencing cell fate specification in the ventral neural tube (16, 17), forebrain neuronal patterning by regulating radial glia cell polarity (18-20), and proliferation of granule neurons precursors in the cerebellum (21-23). Evidence also supports a role of primary cilia in hippocampus-dependent memory formation. For example, neuronal primary cilia are implicated in hippocampal memory by affecting adult neurogenesis (13, 24, 25), and forebrain-specific ablation of primary cilia leads to deficits in aversive learning and memory and novel object recognition (26). However, the function of neuronal primary cilia in postnatal neurodevelopment is poorly understood.

Depending on origination or destination, migrating neurons of developing tissues employ two strategies (27-29): individual or collective migration. Pyramidal neurons in the cortex and hippocampus, which originate from neural tube cells, are individually guided to their destinations by crawling along radial glia fibers (29-31). Individual neuronal migration has three steps for locomotion: leading process extension, nucleokinesis (nuclear translocation), and retraction of trailing process (27). The nuclear translocation of neuronal migration occurs in a saltatory manner, in which the centriole moves forward in the leading process, followed by nuclear translocation that is driven by cytoskeleton dynamics (32-34). The centriole is constantly connected to the nucleus through microtubule network that surrounds the nucleus in a “fork-like” structure (27, 30, 35-37). Hence, centriole and nuclear movements are tightly coupled during the saltatory migration of pyramidal cells. It is worth mentioning that primary cilia possess highly conserved, rigid, 9+0 doublet axoneme architecture (38, 39), which are suited to generate, sense, or engage in cellular mechanical forces (39-45). In this regard, primary cilia, after emanating from centrioles, may mechanically impede saltatory migration during individual neural migration (46).

Accumulating evidence has demonstrated that hippocampal pyramidal neurons exhibit spatially patterned heterogeneity in the adult brain (47-49). Based on the differentiations in molecular, structural, morphological, and physiological features (50-52), the SP of the hippocampal CA1 is subdivided into the deep and superficial sublayers along the radial axis (48, 49). These two sublayers harbor early- and late-

born pyramidal neurons, respectively, which migrate along the radial glia axis from the ventricular zone to the hippocampal plate in a birthtime-dependent inside-out pattern (49, 53). The deep-superficial lamination of SP is thought to be crucial for parallel information processing in the hippocampus (49, 53), because neurons with same birthtime in hippocampal sub-regions (CA1, CA3, and dentate gyrus) connect preferentially with each other and exhibit similar patterns of gene expression (49, 54). The inside-out lamination in the Ammon's horn of the hippocampus shares some similarity to that of the neocortex but has its own features (49, 50). While numerous studies have contributed to unveiling the cellular and molecular mechanisms of neuronal migration during embryonic development for cortical lamination (30, 32, 53, 55-57), it remains elusive how hippocampal pyramidal cells position to the deep and superficial sublayers of the CA1 SP during early postnatal development.

Neuronal primary cilia can be marked by two ciliary proteins, type 3 adenylyl cyclase (AC3) and ADP-ribosylation factor-like 13B (Arl13B) (2). AC3 is abundantly expressed in neuronal primary cilia (1, 2, 58) and represents a key enzyme mediating the ciliary cAMP signaling in the adult brain (59). In contrast, Arl13B generally marks neuronal primary cilia in the developing nervous system (2, 60-62) and primary cilia of non-neural cells (2, 63). Arl13B is an atypical small GTPase that regulates ciliogenesis, ciliary protein trafficking, and the Shh signal pathway (64-68). Arl13B mutations in humans lead to Joubert Syndrome, a congenital ciliopathy featured by cerebellar and cognitive anomalies, renal defects, and other disturbances (69). While Arl13B plays multifaceted roles during embryonic development including regulating interneuron migration (62) and the initial formation of the radial glial scaffold (20), it is unclear if Arl13B affects postnatal neurodevelopment and pyramidal cell positioning in the hippocampus.

To determine if primary cilia regulate pyramidal cell positioning to the sublayers of hippocampal CA1, we examined the morphological dynamics and orientation changes of neuronal primary cilia in the hippocampus and neocortex using AC3 or Arl13B antibodies (2). To confirm cilia orientation, we also used Arl13B-mCherry; Centrin2-GFP double transgenic mice (Arl13B+ mice) (70), in which mCherry labels Arl13B-positive primary cilia, and GFP marks centrioles via fusion with Centrin2, a centriole marker (71). Because Arl13B promotes ciliogenesis (66, 68, 72), this transgenic mouse model also allowed for Arl13B gain-of-function studies to examine the effect of longer primary cilia on cell positioning and centriole migration in the hippocampus during postnatal development. Here we show that hippocampal pyramidal neurons of wild type mice (WTs) do not protrude hair-like primary cilia until pyramidal cells have migrated to SP. Primary cilia in SP undergo marked changes in morphology and orientation from P5-P14, which is a critical period for positioning of pyramidal cells to the deep and superficial sublayers. Interestingly, primary cilia of early-born neurons mostly point to SO, whereas late-

born neurons display opposite cilia orientation, in agreement with the hippocampal inside-out lamination pattern (55). Likely due to delayed ciliation, the centrioles of late-born neurons migrate excessively to pass those of early-born neurons and condense in the edge of SP and SR before primary cilia protrusion and a reverse movement back to the main SP. This "pull-back" movement for cell positioning is different from typical saltatory migration for nucleokinesis during embryonic development. We also discovered that transgenic overexpression of Arl13B promotes primary cilia protrusion several days earlier than WTs. This consequently affects centriole positioning and cilia orientation in the CA1 SP. Together, we conclude that late-born pyramidal cells show a reverse movement during early postnatal development and neuronal primary cilia regulate pyramidal cell positioning to the deep and superficial layers in the hippocampus.

Materials and Methods

Mice

We used WT mice with a C57BL/6j genetic background. The Arl13B-mCherry; Centrin2-GFP mice were purchased from the Jackson Laboratory (Stock No. 027957) and originally had C57BL/6, FVB/N, and BALB/c mixed genetic background. The expression of Arl13B-mCherry and Centrin2-GFP are both driven by the pCAGGs promoter (66, 70, 71). After importing to the lab, we have backcrossed this strain with C57BL/6j mice for more than six generations to obtain uniform C57BL/6j background. The backcrossing has also yielded three separate mouse lines: one keeps as Arl13b-mCherry; Centrin2-GFP double transgenic (Arl13B+ mice), which were used to mark both primary cilia and centrioles; the second becomes Arl13b-mCherry single transgenic mice, which were used for Arl13B gain-of-function studies; the third is Centrin2-GFP single transgenic mice, which labeled centrioles and were served as Control mice for Arl13B+ mice, when we investigated if Arl13B affects cilia orientation and centriole positioning. Mice were maintained on a 12-h light/dark cycle at 22 °C and had access to food and water ad libitum. All animal procedures were approved by the Institutional Animal Care and Use Committee at the University of New Hampshire (UNH).

Brain Tissue Collection

Mice were deeply anesthetized with an intraperitoneal injection of ketamine and xylazine, and then were transcardially perfused with ice-cold 0.1 M phosphate buffer saline (PBS) followed by 4% paraformaldehyde (PFA) in 0.1 M PBS. Young pups (P0 - P7) were directly decapitated using a sharp surgical scissors. Mouse brains were extracted and then placed into 4% PFA overnight at 4 °C. The following day, brains were rinsed in 0.1 M PBS for 30 min at room temperature. P0-P5 mouse brains then were dehydrated by 30% sucrose in 0.1 M PBS overnight at 4°C. Finally, those tissue were embedded in O.C.T resin before being sectioned at -18 °C using a cryostat to a thickness of 30 μm. P7 - P75 mouse brains were coronal sectioned using Compresstome (Precisionary Instruments LLC, NC) to a thickness of 40 - 50 μm.

Immunofluorescence Staining

P0-P5 mouse brains were sliced and mounted on gelatin-coated slices for immunostaining procedure, while P7 – P75 brain sections were sliced and placed in 24-wells plate, staying afloat during the staining procedure. They were washed three times with 0.1 M PBS. Then they were washed in 0.2% Triton X-100 (vol/vol) in 0.1 M PBS for three times for 10 minutes at room temperature. Then they were blocked in

blocking buffer (0.1M PBS containing 10% normal donkey serum (vol/vol), 2% bovine serum albumin (weight/vol), 0.2% Triton X-100 (vol/vol)) for one hour at room temperature. After that, slices were incubated with primary antibodies overnight at 4 °C in blocking buffer. After washing in 0.1 M PBS for three times for 10 minutes, slices were incubated with secondary antibodies for 2 hours at room temperature. Primary antibodies were rabbit anti-AC3 (1:10000, EnCor Biotechnology Inc., #RPCA-ACIII), mouse anti-Arl13B (1:500, UC Davis clone N295B/66), and mouse anti-NeuN (1:500, Millipore-Sigma, MAB377, clone A60). Secondary anti-bodies were Alexa Fluor 488-, 546-, or 647-conjugated (Invitrogen, La Jolla, CA). Finally, sections were counter-stained with DAPI (Southern Biotech™, #OB010020) and images were acquired with confocal microscope (Nikon, A1R-HD), installed in the University Instrument Center at UNH.

Cilia Orientation Measurement

When a single primary cilium in WT mice was measured, the relative thinner axoneme was defined as the tip and the opposite site as the base. For Arl13B-mCherry & Centrin2-GFP transgenic mice, the location of the primary cilium base was the same as Centrin2-GFP. The tails of most primary cilia in WT mice were straight and easy to determine their angles. However, primary cilia in the Arl13B-mCherry & Centrin2-GFP transgenic mice were much longer and showed kinks in their axoneme (66). For those primary cilia, the initial part (~2 µm from the base) was used for determining the angle of those primary cilia. Fiji was utilized to measure the orientation of the single primary cilium. Four steps were used to complete a measurement. 1) First, the angle tool was selected among icons showed in the main window. 2) Then, the shift button on the keyboard was held, while left clicking the mouse meanwhile to draw a line (always from the right to left and parallel to the external capsule) to the location of the base of the primary cilium. 3) Afterwards, the shift button was released, and the mouse was left clicked to draw a line from the base to the tip of the primary cilium. 4) Lastly, while holding the control button and selecting "M" on the keyboard, the angle would jump out in a separate window. To measure the next primary cilium, steps 2-4 were repeated. Acquired data were finally exported as an excel file and then to a MATLAB program, which was used to generate polar plots.

Primary Cilia Length Measurement

We measured the length of primary cilia based on published methods (73), with modifications. The freehand line tool within Fiji (ImageJ) was used to measure cilia length from the base of axoneme to the distal tip. 40-µm Z-stack confocal images in Fig. 2 were used for both of adult WT and Arl13B+ mice. 20-

μm Z-stack confocal images were used for Fig. 1, Fig. 4, P3, P7, P10, and P14 Arl13B+ mice. Confocal images of 20 μm Z-stack were used for Fig. 7.

CA1 SP Thickness Estimation

Confocal images of 20 μm Z-stack were used for quantifying CA1 SP thickness for both WT, Arl13B+ mice and Control mice. The straight line tool within Fiji was used to measure CA1 SP thickness from the top of SP to the bottom of SP based on nucleus staining (74). Because the nuclei at the top and bottom edge of SP are not aligned to a straight line, this causes some variation of SP thickness. For young adult mice, we chose coronal sections at -1.9 mm posterior to Bregma to measure CA1 SP thickness. For young pups, we measured the thickness based on selected slices with hippocampal anatomic geometry similar to adult hippocampal sections. We acknowledge that our estimation method has limitations and stereotaxic accuracy needs to be improved. Nevertheless, it is known (74) that CA1 SP thickness decreases markedly with age, particularly during the first two weeks. We present CA1 SP thickness changes with ages to demonstrate that hippocampal pyramidal cells maintain certain movement or re-positioning postnatally, yielding significant changes during early postnatal period (before P14) and mild adjustment afterwards.

Quantification of nucleus density, centriole density, and ratio of centriole to nucleus (C/N Ratio)

A 70 μm x 70 μm square box in SP was used for one single area quantification. The freehand line tool within Fiji was utilized to draw a line that matched the margin of the nucleus at the bottom of SP in the chosen box. This line was then vertically moved down 15 μm (to the SR direction) and up 15 μm (to the SO direction). The panel between two lines was defined as the bottom panel of SP for quantifying nucleus, centrioles, and C/N Ratio. The top line at the bottom panel of SP was further moved up 30 μm (to the SO direction). The area between the two lines (having a width of 30 μm) was defined as the middle panel of SP for the quantification of nuclei and centrioles. Since many centrioles were found to be clustered in the SR particularly in ARl13B+ mice, we also included a 15-μm-width area in the SR that was next to SP for quantification (Fig. 5I). Two Centrin2 dots were counted as one pair of centrioles, one DAPI separate round region were counted as one nucleus.

Statistical and Software

Data were analyzed with Fiji, GraphPad Prism and MATLAB. Data was considered as statistically significant if $p < 0.05$ and values in the graph are expressed as mean ± standard error of the mean. Statistical analyses were conducted using ANOVA for multiple group comparison or Student's T-test with a two-tailed distribution, as appropriate. N.S., Not Significant; * $p < 0.05$; ** $p < 0.01$; *** $p < 0.001$.

Results

Neuronal primary cilia of early- and late-born hippocampal pyramidal cells exhibit opposite orientation.

The SP of hippocampal CA1 consists of deep- and superficial-sublayer, inhabited by early- and late-born pyramidal cells, respectively (47-49, 55). It is not well understood how early- and late-born pyramidal cells position themselves into two sublayers postnatally. We performed immunofluorescence staining using AC3 and Arl13B antibodies to examine the morphological changes of neuronal primary cilia in SP during postnatal development. We found that primary cilia orientation in SP undergoes marked changes during early postnatal development (Fig. 1A-D). Until P7, AC3- or Arl13B-positive neuronal primary cilia were barely detected in SP of WT mice (Fig. 1A). At P10, neuronal primary cilia protruded and became prominent, with many clustered at the edge of SP and SR (Fig. 1A). They exhibited opposite orientation: the axoneme of primary cilia at the bottom (superficial sublayer) mostly pointed in the SR direction, whereas those at the top (deep sublayer) oriented to the SO direction. From P10 to P14, cilia orientation underwent a drastic change, ~40% of cilia pointed to SO (north) at P10, while at P14 nearly 20% of cilia pointed to SO (Fig. 1D). At P14, superficial-sublayer neuronal cilia occupied the major space of the SP, and the axonemes of primary cilia almost uniformly pointed in the SR direction. Deep-sublayer neurons were then squeezed to a thin layer on the top and their cilia maintained towards SO. Afterwards (e.g., at P40 and P75), cilia orientation did not change much (Fig. 1C-D), except for becoming less aligned with the radial axis (Fig. 1A). However, primary cilia of superficial-sublayer neurons were still aligned with the radial axis and oriented toward SR. Polar plots and histogram plot in the Fig. 1C demonstrate changes in cilia orientation from P10 to P75. It is noteworthy that the laminar thickness of SP decreased significantly from P3 to P14 and reached a steady-state someday between P14 and P40 (Fig. 1E-F), suggesting that pyramidal cells continue to adjust their position postnatally, which consequently condenses cell density and CA1 lamina thickness.

To confirm if primary cilia with opposite orientation come from early- and late-born pyramidal neurons, respectively, we performed immunofluorescence staining using an antibody of calbindin, which is a marker for late-born neurons in the dorsal hippocampal CA1 after P20 (49, 75). Fig. 1G shows that primary cilia of calbindin-positive neurons in the superficial sublayer largely point in the direction of SR, whereas calbindin-negative neurons' primary cilia generally orient toward the SO direction, supporting the notion that early- and late-born pyramidal neurons exhibit opposite cilia orientations. To demonstrate early- and late-born neuron distribution in SP, we include *in situ* hybridization (ISH) results of Col11a1 and Htr1a adopted from Allen Brain Atlas (https://mouse.brain-map.org/). Col11a1 is a marker of early-

born pyramidal neurons (48), while Htr1a is selectively expressed in late-born neurons (49). ISH results show that Col11a1 mRNA is mostly detected in the deep sublayer, with a small fraction also distributed to the superficial sublayer (Fig. 1H). Htr1a mRNA is identified largely in the superficial sublayer, whose staining signals do not cover all areas of the superficial sublayer (Fig. 1I). This suggests that although early- and late-born pyramidal neurons markedly differentiate in function and morphology and inhabit the deep- and superficial-sublayers, respectively, there is no clear bound to physically separate two groups of neurons in CA1 sublayers. Together, these data indicate that primary cilia of early- and late-born hippocampal pyramidal neurons exhibit opposite orientation, suggesting a role of neuronal primary cilia in pyramidal cell positioning during early postnatal development.

Arl13B regulates neuronal ciliogenesis, cilia orientation, and pyramidal cells positioning to CA1 sublayers.

We observed that neuronal cilia marker AC3 expression in pyramidal cells in the CA1 remains relatively stable after P10 (Fig. 1A)(2). In contrast, Arl13B started to emerge at P7 with staining identified mostly in SP bottom (Fig. 1A top). At P10, Arl13B expression reached a high level in the SP, particularly strong at SP bottom, then decreased at P14 and further reduced at P40, and became very weak in adulthood (Fig. 1A). Arl13B high expression appears to occur within the same time-window as pyramidal cell positioning and neuronal maturation (or development of synaptic connectivity) from ~P5 to P14 (76-79), suggesting a role in neuronal positioning. Arl13B is a ciliary small GTPase that modulates ciliogenesis, interneuron migration, and maturation (20, 67, 68). We have previously reported that Arl13B+ mice have much longer neuronal primary cilia in the hippocampus (66). Although Arl13B+ mice display a high percentage of seizure phenotype partly due to their hybrid FVB background (66), we overcame this limitation by backcrossing this strain with C57Bl/6J mice for over six generations. It turned out that Arl13B+ mice in C57Bl/6J background do not exhibit seizure phenotypes. We found that neuronal primary cilia are the longest in the hippocampal CA1, compared to several other brain regions such as CA3, dentate gyrus, cortex, and amygdala in adults (Fig. 2). Moreover, we compared the cilia length of Arl13B+ adult mice with WT adult mice and found that the effect of Arl13B on elongating cilia length was very strong in the CA1, and much weaker in other regions including amygdala and cortex (Fig. 2). This highlights an important role of Arl13B in regulating neuronal cilia length, particularly in the CA1.

To determine if Arl13B overexpression affects cilia orientation, we next characterized dynamics of cilia orientation during postnatal development using Arl13B+ mice. First, we found that at P7 neuronal primary cilia were prominent in Arl13B+ mice (Fig. 3A), which was different from WT mice (Fig. 1A).

Deep-sublayer neuronal primary cilia largely pointed to the SO direction, whereas primary cilia of superficial-sublayer neurons clearly show opposite cilia orientation (Fig. 3A). Second, immunostaining images from P7 to ~P75, polar and histogram plots of cilia orientation indicate that primary cilia of Arl13B+ mice underwent drastic changes in orientation from P7 to P14 and mild changes from P14 to P75 (Fig. 3A-C), similar to WT mice. This suggests that the time-window before P14 is crucial for changes in cilia orientation. Third, overexpression of Arl13B affected the percentage of primary cilia having SO or SR orientation: at P14 and P40, more primary cilia pointed to the north in Arl13B+ mice than WT mice (Fig. 3D). It is noteworthy that at P7 neuronal primary cilia in WT mice were not expressed, but Arl13B+ mice have a large portion of cilia pointing to the north (Fig. 3A-C). Fourth, the lamina thickness of CA1 SP decreased significantly from P3 to P14, and more at ~P75 (Fig. 3E-F), suggesting that CA1 neurons continuously adjust their position. Lastly, we also used calbindin staining to verify that primary cilia with opposite orientation were indeed from early- and late-born pyramidal neurons, respectively (Fig. 3G-H). These data demonstrate significant changes in cilia orientation and strong effects of Arl13B in modulating CA1 cilia orientation during early postnatal development.

Drastic changes in cilia morphology and orientation were found before P14 in both WT and Arl13B+ mice (Fig. 1&2), which was concurrent with the high expression of Arl13B in the CA1 (Fig. 1A) and with neuronal positioning time-window. This suggests a role of Arl13B in pyramidal cell positioning by modulating ciliogenesis. To determine if Arl13B affects ciliation timing and pyramidal cell positioning to deep- and superficial sublayers of SP, next we examined changes in cilia morphology and orientation as well as centriole distribution in the CA1 from P3 to P14. We found that overexpression of Arl13B not only elongated primary cilia, but also affected the timing of ciliation (Fig. 4A). Arl13B+ mice started to express primary cilia in the deep sublayer as early as P3, all of which pointed to SO (Fig. 4A). At P5, more primary cilia emerged from deep-sublayer neurons, and some from superficial-sublayer neurons (Fig. 4A). At P7, primary cilia of deep-sublayer neurons became pretty long, while primary cilia of superficial-sublayer neurons were not fully elongated, with many remained short or dot-shaped at the bottom of SP (Fig. 4A). We quantified the cilia length of deep- and superficial sublayer at P3, P7, P10, and P14. Clearly, the cilia length of deep-sublayer neurons was much longer than that of superficial-sublayer neurons from P3 to P10, but at P14 both groups of neuronal cilia reached a plateau level (Fig. 4B). These data demonstrate that the expression of primary cilia of deep-sublayer (early-born) neurons are earlier than superficial-sublayer (late-born) neurons in Arl13B+ mice. In contrast, hair-like primary cilia were barely detectable at P5 in the hippocampal CA1 of WT mice (Fig. 4A). At P7 they still did not express many hair-like primary cilia, while AC3 staining become a bit more obvious in the deep sublayer than superficial

sublayer. At P9, WT mice started to express many short cilia in the main SP, and at P10 cilia become longer, however, these cilia distribution did not display a deep-superficial sublayer distinction as clearly as that of Arl13B+ mice at P7 or P10 (Fig. 4A). These images indicate that Arl13B promotes earlier primary cilia protrusion and affects cilia distribution in the CA1.

The results that primary cilia of early-born neurons emerge earlier than that of late-born neurons and both reach full length at P14 raised the questions if early-born pyramidal neurons mature earlier than late-born pyramidal neurons and if neuronal maturation and ciliation occur within the same time-window. To examine if there is a birthtime-dependent maturation in SP sublayers, we employed an antibody of NeuN, a protein marker for matured pyramidal neurons (80, 81), in our immunostaining assay. Fig. 4C shows that the expression of NeuN at P1 was not detected, except for some weak staining in the deep sublayer of SP. At P5, NeuN expression became stronger in the deep sublayer, but not much in the superficial sublayer. At P7, the superficial sublayer started to have higher NeuN expression, and at P14, NeuN was abundantly expressed in both deep- and superficial-sublayers. This "first deep - then superficial" sequential NeuN expression pattern indicates an order of birthtime-dependent neuronal maturation in the CA1. To determine if glutamatergic synaptic markers (indicative of synaptic connectivity) show a similar pattern, we checked Allen Brain Atlas Developing Mouse Brain Database (https://developingmouse.brain-map.org/). Indeed, we found that many synaptic marker proteins of glutamatergic synapses including Shank3 (Fig. 4D), and Homer-1 (Fig. 4E), as well as Camk2a, PSD-95, Synapsin-1, Syntaxin 1, and Neurexin 1 (not shown here, but their ISH data are available in the Atlas), display a similar sequential expression pattern: first expressed in the deep sublayer of SP at P4 or so, then extended to the superficial sublayer and reached full expression at P14 (Fig. 4D-E). This expression sequence is in accordance with the order of primary cilia protrusion from P5 to P14 first in the deep and then superficial sublayers of the CA1 in Arl13B+ mice.

We acknowledge that WT mice have dot-shaped primary cilia in the superficial sublayer of SP before P9 (Fig. 4A). Nevertheless, it is known that several steps of ciliogenesis occur under the plasma membrane and before cilia protrusion (82, 83). In addition, we did detect a few SO-pointing primary cilia in the deep sublayer as early as P5 (Fig. 4A) and at P3 (not shown) in WT mice, indicating that neuronal ciliogenesis, albeit very weak, does occur in WT mice before P9. Arl13B overexpression promotes earlier cilia protrusion and amplifies cilia expression, which allowed us to visualize hair-like primary cilia and reveal this new ciliation pattern. Interestingly, the timing of ciliation and neuronal maturation is not solely determined neurons' birthtime. For example, CA3 neurons are born around the same time as CA1 neurons and CA3 pyramidal layer also follows an inside-out lamination pattern (55), although there are other types

of neurons migrating to CA3 (50). We found that the hippocampal CA3 of WT mice had abundant expression of primary cilia at P7 (Fig. 4F), whereas CA1 did not (Fig. 4A), indicating that CA3 protrudes primary cilia earlier than CA1. Likewise, hippocampal CA3 pyramidal neurons mature earlier than CA1 neurons, as evidenced by strong expression of several glutamatergic synapse marker proteins including Camk2a and PSD-95 in the CA3 at P4 (Fig. 4G), in contrast to their very weak and deep sublayer-restricted expression in the CA1 (Fig. 4G). ISH data of other glutamatergic synapse markers (available at https://developingmouse.brain-map.org/) also exhibit similar patterns. These data support the argument that hippocampal neuronal ciliation is closely related to neuronal maturation, not strictly to birthtime. Together, we conclude that the neuronal ciliation in CA1 sublayers occurs from P5 to P14, concurrent with neuronal and synaptic maturation in an order of "first deep - then superficial".

After being clustered at SP bottom, a reverse movement of centriole/cilia is deployed to position late-born pyramidal cells to the superficial sublayer of SP.

We further observed that cilia density in the main SP of Arl13B+ mice at P7 was very low, and obviously there were more nuclei than primary cilia (Fig. 4A). A large fraction of cilia/centrioles was instead congregated at SP bottom, and not many cilia were found in the middle panel of SP (Fig. 4A). However, a few days later at P14, cilia distribution became more even in SP (Fig. 3A). This suggests the possibility that the centrioles of late-born pyramidal neurons migrate excessively to reach and cluster at SP bottom before re-distribution.

To test it, we quantified and compared nucleus density, centriole density, and the ratio of centriole to nucleus (C/N Ratio) in the CA1 SP at P3, P7, P10 and P14 using both Arl13B+ and Control mice (Fig. 5A-B). Comparison of Arl13B+ with Control mice also enabled us to unveil the effects of Arl13B overexpression on centriole positioning. For better quantification, we artificially separated confocal images of SP into top, middle, and bottom panels (as shown in Fig. 5I). We also included a section of SR (15 μm) in the quantification because some centrioles also reached SR (Fig. 5I). First, we discovered that Arl13B+ and Control mice do not show significant differences in nucleus density at the middle and bottom panels from P3 to P14 (Fig. 5A-B), indicating that neurons' nuclei are evenly distributed in the SP during this period. However, centrioles were highly condensed at SP bottom at P3 and P7 in both Arl13B+ and Control mice (Fig. 5A-B), because the C/N Ratio in SP bottom and SR were much higher than 1 (Fig. 5D). Second, centriole density at the bottom panel was much higher than at middle panel at P3 and P7 in both Arl13B+ and Control mice (Fig. 5C). However, afterwards at P10 and P14, centrioles show a relatively even distribution in the SP (Fig. 5A&C). Consistently, C/N Ratio in both Arl13B+ and Control mice at P3

were about 2.5, but it gradually decreased to 1 at P14 (Fig. 5D). Third, Arl13B+ mice have a lower centriole density at the middle panel than Controls at P3 and P7 (Fig. 5C), but their C/N Ratio in SP bottom and SR were much higher than Control mice at P7 (Fig. 5D), indicating a higher enrichment of centrioles in SP bottom in Arl13B+ mice than Control mice. This result also demonstrates an effect of Arl13B on centriole positioning or distribution in the SP.

The changes in centriole distribution from P3 to P14 also suggest that there was a reverse movement (from SP bottom back to main SP) for centriole positioning. To verify this, we took and presented confocal images of both Centrin2 and Arl13B. Indeed, at P7 in Arl13B+ mice, cilia density in the upper part of SP was very low, while centrioles and short primary cilia were highly condensed at SP bottom (Fig. 5E). At P10, neuronal primary cilia became much longer. Some centrioles/cilia became well-aligned with radial glia fiber, while others still clustered at SP bottom (Fig. 5E), suggesting that some neurons started to move toward the north (SO direction), and centrioles took the lead, followed by hair-like cilia tail (Fig. 5E). At P14, long cilia occupied the major space of SP, and their primary cilia almost uniformly pointed to the SR direction (parallel to the radial glia fiber). There were no more centrioles/cilia clustering at SP bottom (Fig. 5E). These data indicate that centriole and cilia move reversely to re-distribute from the bottom of SP to the main SP. We quantified cilia orientation of the upper part of SP. Consistently, the upper part of SP originally only had SO-pointing cilia at P7. Due to this "pull-back" cilia/centriole movement, more south-oriented cilia gradually moved to main SP from P7 to P14, the upper part of SP subsequently contained more south-oriented cilia (Fig. 5G-H). Together, we conclude that the cilia/centrioles of late-born pyramidal neurons move against the saltatory migration direction to position to the superficial sublayer. We name this phenomenon "reverse movement", as contrast to typical forward saltatory migration. A schematic model in Fig. 5F depicts the cilia orientations and the direction of the reverse movement. Our data also suggest that the reverse movement of late-born neurons from P7 to P14 may indirectly affect late-born neurons' maturation or their development of synaptic connectivity, which occurs several days later than early-born neurons in the CA1 (Fig. 4C-E).

Late-born cortical pyramidal neurons also undergo a reverse movement and protrude primary cilia later than early-born neurons.

Hippocampal CA1 and the neocortex share similarities in their neuronal migration mode in the embryonic stage (30, 50, 84). For instance, they consist of the same originated early-born and late-born pyramidal neurons, which inhabit the deep- and superficial sublayer, respectively (49). Next, we asked if postnatally primary cilia of cortical pyramidal neurons exhibit similar pattern to that of hippocampal CA1. We found

that in terms of cilia orientation, neuronal primary cilia in cortical layer II-III (superficial sublayer) most pointed to the pial surface both at P14 and P40 (Fig. 6A), consistent with results in the CA1 superficial sublayer and with previous report (85). However, late-born pyramidal neurons in cortical Layer V (deep sublayer) did not exhibit opposite cilia orientation to early-born neurons (Fig. 6A). Instead, most of primary cilia of Layer V neurons still pointed to the pial surface, although Layer II neurons had a higher percentage of cilia pointing to the pial surface (Fig. 6B). Cortical Layer VI does not harbor many pyramidal neurons and their cilia orientation was different from Layer II/III and Layer V (Fig. 6C). These data indicate that early- and late-born cortical pyramidal neurons have the same cilia orientation, which is different from that of CA1.

To determine if cortical pyramidal neurons are subjected to reverse movement as late-born hippocampal neurons before P14, we examined centriole/nuclei distribution pattern in the superficial sublayer (Layer II/III) of the neocortex at P3 and P14 (Fig. 7A). For better quantification, we drew top and middle panels on the images of Layer II/III to quantify cilia and nuclei density. We found that the density of centrioles (Fig.7B) and nuclei (Fig.7C) at the top panel were higher than those at the middle panel at P3. However, at P14 both centriole and nuclei density between two panels showed no significant differences. These data indicate that the densities of centrioles and nuclei in Layer II/III have changed from compact and uneven at P3 to sparse and even at P14. This strongly suggests that there is a reverse movement from the top to middle panel, which distributes centriole/nuclei evenly at P14 (Fig. 7B-C) and makes neuronal cilia pointing to the pial surface (Fig. 6A). However, the C/N ratios were near 1 and there were no significant differences between P3 and P14 and between the top and middle panels (Fig. 7D), suggesting that there is no excessive clustering of centrioles at Layer II/III of the neocortex, which is different from the case of hippocampal CA1.

To determine if cilia expression of cortical neurons similarly exhibit an order of "first deep - then superficial", we compared the ciliation timing of early- and late-born cortical neurons. We found that at P3 and P7 primary cilia of early-born cortical neurons were much longer than those of late-born neurons (Fig. 7E-H). These data indicate that early-born cortical neurons express primary cilia earlier than late-born neurons. Consistently, ISH results from Allen Brain Atlas also demonstrate that Shank3 and Homer1 display similar sequential pattern in the neocortex: first expression in the cortical deep sublayer at P4, then extended to the superficial sublayer at P14 (Fig 4D-E). Other synaptic markers, such as PSD-95 and syntaxin-1, also exhibit similar patterns (https://developingmouse.brain-map.org/). Therefore, this maturation sequence of pyramidal neurons in cortical layers is similar to that of hippocampal CA1,

supporting the notion that neuronal ciliation is related to cell positioning, reverse movement, and neuronal maturation in both hippocampal and cortical sublayers.

Discussion

This study provides the first evidence demonstrating that neuronal primary cilia play an important role in postnatal neurodevelopment by modulating pyramidal cell positioning to the deep and superficial sublayers. (1) The axoneme of primary cilia of early-born neurons point to SO, whereas those of late-born neurons display opposite cilia orientation. Neuronal primary cilia in the hippocampal SP undergo drastic changes in orientation and morphology from P5-P14, concurrent with pyramidal cell positioning to the deep and superficial sublayers. (2) Transgenic overexpression of Arl13B not only elongates primary cilia and promotes earlier cilia protrusion, but also affects centriole migration and cilia orientation in the CA1 SP. (3) We identified a novel migration mode of centrioles/cilia during cell positioning, which is different from typical saltatory migration for nucleokinesis. After reaching SP bottom, centrioles of late-born neurons protrude primary cilia and then undergo a reverse movement back to the main SP, which makes cilia axoneme point to SR. (4) The ciliation of pyramidal neurons in the neocortex also coincides with neuronal positioning time-window, but neuronal primary cilia in the deep and superficial sublayers exhibit the same orientation. (5) After migrating to Layer II/III of neocortex and congregating there at P3-P7, late-born neurons start to express neuronal primary cilia, followed by a reverse movement to disperse cell density. The reverse movement helps explain why neuronal primary cilia in Layer II/III point to the pial surface.

P5-P14 is a critical developmental time-window for ciliation, pyramidal cell positioning to CA1 sublayers, and neuronal maturation.

It has been documented that pyramidal neurons in the mouse hippocampus are generated during embryonic days (E) 12 - 18 (86, 87), and their generation peaks between E14 and E16 (84, 86, 88). After early- and late-born pyramidal neurons migrate from the ventricular zone or sub-ventricular zone to the hippocampal plate, early-born neurons position to the deep sublayer of SP and late-born neurons migrate to pass early-born neurons and reside in the superficial sublayer (50, 89). This is so called birthdate-dependent inside-out lamination pattern (49, 55). Although embryonic developmental profiling of early- and late-born neurons have been well characterized (47-49, 89), how those neurons postnatally adjust their final positions in the CA1 sublayers and settle down to develop synaptic connectivity are poorly understood. It is known that excitatory synaptic connectivity in the mouse hippocampus develop and

neuronal become matured in the first two weeks of life (77-79, 90), however, it is unknown why CA1 pyramidal neurons need to wait until P14 to construct stable synapses, and if neuronal primary cilia engage in the neuronal positioning and maturation process. Our data demonstrate that ~P5 to P14 is a critical period for early- and late-born pyramidal neurons to position to the deep- and superficial sublayers in the CA1, respectively. First, primary cilia undergo drastic changes in morphology and orientation from P5-P14 (Fig. 1A, 2A, 3A). The thickness of SP lamina decreases significantly from P3 to P14, concurrent with cilia emergence and marked changes in cilia orientation (Fig. 1D and 3C). Second, Arl13B+ mice start to express primary cilia first from early-born neurons at P3. Several days later at P7, late-born CA1 neurons of Arl13B+ mice started to express primary cilia. After P14, both cilia length and orientation do not change much, reaching a steady state. In addition, centriole distribution in SP changes from clustering at the edge of SP and SR at P3-P7 to even distribution in the main SP at P14 (Fig. 5A-D). Together, cilia length and orientation, CA1 lamina thickness, and centriole/cilia distribution in the SP are all subjected to marked changes from P5-P14 and reach a plateau at P14. These changes additionally show an order of "first deep - then superficial". Likewise, neuronal maturation also shows a similar pattern. For example, NeuN, a marker for matured neurons (80), starts to brightly express only in early-born neurons in SP at P5, followed by late-born neurons at P7, and reach abundant expression in both early- and late-born neurons at P14 (Fig. 4C). Consistently, many synaptic markers of excitatory neurons including Shank3 (Fig. 4D) and Homer1 (Fig. 4E), as well as Camk2a, PSD-95 (Fig. 4G), Synapsin-1, Syntaxin 1, and Neurexin 1 (ISH data available in the Allen Brain Atlas Developing Mouse Brain), first emerge from early-born neurons in the CA1 around P4, then extend to late-born neurons, reaching a plateau in both early and late-born neuron at P14. This indicates that early-born CA1 pyramidal neurons mature earlier than late-born neurons.

Interestingly, CA3 pyramidal neurons mature several days earlier than CA1 pyramidal neurons (Fig. 4G), evidenced by the expression of synaptic marker proteins, such as Camk2a, PSD-95, Synapsin-1, Syntaxin 1, and Neurexin 1 in the Allen Brain Atlas Developing Mouse Brain. We have discovered that CA3 express primary cilia earlier than CA1 at P7 WT mice (Fig. 4F). This supports the notion that primary cilia expression is closely related to neuronal maturation. These data raise the interesting question why late-born CA1 pyramidal neurons need to wait until P14 to become matured? We reason this is probably because the reverse movement of CA1 late-born neurons occurs from P7 to P14. We show that the CA1 lamina thickness can greatly reduce from 90 μm to ~70 μm from P7 to P14 (Fig. 1) and reach a steady-state level of 60 μm some day between P14 and P40, After P40, CA1 SP thickness is only subject to very mild changes, so does changes in cilia orientation (Fig. 1&3). Because late-born neurons undergo striking

reverse movement (over a distance of 10 μm to 30 μm) from P7 to P14, it could destabilize the cytoskeleton of dendrites and synapses, affecting the stability of synapses after being formed. This speculation is in line with numerous reports showing that CA1 glutamatergic synapses before P14 are silent or labile, and their electrophysiological features are different from mature synapses after P14 (77-79, 91, 92). Likewise, cortical Layer II/III late-born neurons also mature later than Layer V early-born neurons (Fig 7D-E) (data are available in the Allen Brain Atlas Developing Mouse Brain). Our data indicate that late-born cortical neurons also have a reverse movement before P14 (Fig. 7A), and their late maturation could also be, at least in part, explained by their reverse movement. Collectively, this study and protein expression analyses of Allen Brain Atlas demonstrate that ~P5 to P14 represents the critical period to position early- and late-born neurons to the deep- and superficial-sublayer of hippocampal CA1, respectively. Early-born neurons mature earlier, and the reverse movement of late-born neurons likely delays their final positioning, neuronal maturation or construction of synaptic connectivity in the superficial sublayer. This line of research warrants future studies, and revealing this developmental pattern will help understand how CA1 pyramidal cell heterogeneity of two sublayers enables parallel information processing in neural networks, affecting learning and memory formation.

Postnatal development of CA1 sublayers is regulated by ciliation timing

While pyramidal neurons in the hippocampal CA1 and neocortex are arranged in an inside-out layered structure, cortical lamina volume expand significantly during postnatal neurodevelopment (93), while the CA1 layer is gradually condensed. Although studies have demonstrated that the thickness difference may be caused by different migration mode in the embryonic stage (49), it is not very clear how the SP is further subdivided into the superficial and deep sublayers in a very thin laminar structure.

This study has examined changes in cilia morphology and orientation in two sublayers of CA1 during postnatal development. The commonalities and difference of the cilia expression pattern identified in this study might partially explain this question. First, we found that early-born neurons exhibit longer cilia length than late-born neurons at P3 and P7 in the CA1 SP and the neocortex (Fig. 4A-B, 7E-H). This cilia length and ciliation timing difference in each sublayer is consistent with the expression pattern of NeuN staining and synapses makers (Fig. 4C-E). Our data suggest that ciliation timing is closely related to neuronal maturation in the deep and superficial sublayers. Second, we have identified an opposite cilia orientation in pyramidal neurons in the deep and superficial sublayers of CA1 SP (Fig 1A and 3A), whereas primary cilia in cortical sublayers show the uniform orientation (Fig. 6A). Uniformed cilia orientation is the same direction of apical dendrite of cortical pyramidal neurons, but only pyramidal

neurons in the SP superficial sublayer points in the apical dendrite direction, deep-sublayer neurons point in the opposite direction (Fig. 3A). This distinct difference of primary cilia orientation between the CA1 SP and neocortex supports the possibility that primary cilia regulate the postnatal development of SP. For unknown reasons yet, they are designed to orient oppositely in early- and late- born neurons to promote separation of the deep- and superficial-layer in the CA1 SP. In addition, Arl13B, which is highly enriched in primary cilia during early neurodevelopment, elongates cilia length in CA1 pyramidal neurons in Arl13B+ mice (Fig. 4). Their early-born neurons show several days earlier neuronal cilia expression than late born neurons, which may impact the moving dynamic of neuronal migration and cause centriole distribution variation (Fig. 5A-D). In our working model (Fig. 5F), we propose that the ciliation timing is critical for the modulating effect of primary cilia on cell positioning. Primary cilia of early-born neurons (with early ciliation) likely impede saltatory migration and stabilizes neurons in a specific location, while late-born neurons (with delayed ciliation) can migrate excessively to reach SP bottom, which consequently promotes the sorting of early- and late-born neurons to the deep and superficial sublayers, respectively. Arl13B overexpression promotes the early expression of primary cilia of early-born neurons, which may impede centriole migration of early-born neurons toward the SR direction. This enhances the separation of centrioles/cilia of early-born neurons with those of late-born neurons (Fig. 4A).

Additionally, this study has revealed several interesting distinctions between early- and late-born pyramidal neurons in the CA1: Early-born pyramidal neurons express primary cilia earlier; their cilia point to SO; their synapses mature earlier; they complete positioning earlier and do not experience a reverse movement. In contrast, late-born pyramidal neurons migrate a longer distance and their centrioles reach and cluster at SP bottom; they express primary cilia several days later, which point to SR; late-born neurons are subjected to a reverse movement; and they complete cell positioning later, and consequently late-born neurons (and their synaptic connectivity) mature several days later.

Primary cilium is likely to orient in a specific direction to modulate early- and late-born neurons positioning

The centrosome/centriole, as the microtubule-organizing center, directs cellular microtubule dynamics that couple to nuclear translocation during individual cell migration (30, 33, 34, 94). Polarized centriole positioning is found to be important for properly oriented cell division, cilia positioning, and cell migration (95). Based on our data, we propose a working model, in which primary cilia protrusion affects pyramidal cell positioning to the deep and superficial sublayers of SP by modulating centriole migration and positioning (Fig. 5F). After early- and late-born pyramidal neurons migrate to reach the SP, primary cilia

first protrude from early-born pyramidal cells, pointing towards SO (Fig. 1-4), which is opposite to the pyramidal neuron migration direction (from SO to SR). This rigid surface protrusion may slow down the saltatory migration of early-born neurons and help hold them in the deep sublayer. On the other hand, the protrusion of primary cilia of late-born neurons occurs several days later than early-born neurons (Fig. 4). Likely because of delayed cilia protrusion, late-born neurons excessively migrate a longer distance than early-born neurons to reach the SP bottom, where their centrioles start to protrude primary cilia. Afterwards, late-born neurons undergo a reverse movement back to the main SP (Fig. 5E). We believe that both the cell body and cilia/centrioles of late-born neurons move backwards, because the lamina thickness of CA1 SP decreases significantly from P3 to P14. We postulate that early-born neurons most likely position and mature from P4-P7, while late-born neurons reversely migrate toward the north from P7-P14, which consequently condense the SP. Primary cilia point in the opposite direction as early- and late-born neurons migration direction, suggesting that the primary cilium is very likely to serve as a mechanical anchor for adjusting cell positioning and movement. It is not uncommon for primary cilia to engage in mechanical forces (39-45). For example, a recent study has shown that mechanical strain controls the length, motility, and planar position of primary cilia, affecting the determination of left-right body axis during gastrulation (96). We also have shown that olfactory cilia can sense mechanical force of airflow to regulate olfactory perception (97). Given unique mechanical features of primary cilia, we propose that primary cilia protrusion may function like "mechanical anchor of centrioles" to regulate centriole positioning in the cell and affect pyramidal cell positioning to CA1 sublayers. Regarding cortical Layer II/III (superficial sublayer) and Layer V (deep sublayer) excitatory neurons that show the same cilia orientation, we postulate that both are subjected to the same direction of reverse movement for neuronal positioning. Nevertheless, it requires more evidence to support such an interpretation.

In summary, this report presents the first evidence demonstrating that neuronal primary cilia regulate pyramidal cell positioning to CA1 sublayers. We also document that the reverse movement of late-born neurons from the bottom of SP to the main SP is crucial for the establishment of the laminar structure of hippocampal CA1, which may indirectly affect the maturation or synaptic connectivity of late-born neurons.

Figure Legends

Fig. 1. Opposite primary cilia orientation in the deep and superficial sublayers of hippocampal SP. ***(A-C)*** Opposite orientation of primary cilia in the hippocampal SP of WT mice. ***(A)*** Co-immunofluorescence staining using AC3 (red) and Arl13B antibody (green) on hippocampal slices from

P7 to ~P75. Cilia orientations exhibit marked change with ages from P10 to ~P75. Scale bars: 10 µm. ***(B)*** A diagram of cilia orientation measurement in the dorsal hippocampal CA1. Cilia shown in SP are posited in the polar plot on the right. Polar plots analyses were performed to determine primary cilia orientation distribution. The numbers (0-360º) on the out circle denote the degree of cilia orientation relative to the external capsule, and the numbers on concentric circles are the percentage of cilia orientation at specific angles. ***(C)*** Polar plots and histogram plots showing cilia orientation pattern and their corresponding percentages. Most primary cilia axoneme point to the SR direction (180º - 360º) in polar plots (Left). The histogram plots (binned in 10-degree intervals, Right) present the percentage of cilia at different angles. The degrees in polar plots were converted to histogram plots by subtracting 180º. **(D-F)** Changes of cilia orientation coincide with the decrease of SP thickness during postnatal development. ***(D)*** Statistical data showing the percentage of north-oriented cilia (pointing to SO direction). Each triangle represents one location in SP for quantification. The percentage of north-oriented cilia decreased significantly from P10 to P14. N.S., not significant, *** $p < 0.001$, One-way ANOVA test. ***(E)*** The thickness of SP lamina in the hippocampal CA1 decreases significantly from P3, P5, P10, P14, to P40 and ~P75. *** $p < 0.001$, One-way ANOVA Test. ***(F)*** Co-immunostaining of AC3 (red) with Arl13B (green) and DAPI (blue) on brain slices at P3, P14, and ~P75. Primary cilia orientation changed from well-aligned (P14) to less ordered (~P75). Scale bars: 20 µm. ***(G)*** Immunofluorescence staining using AC3 and calbindin antibodies. Primary cilia of calbindin-positive neurons at P40 mostly pointed in the SR direction, while calbindin-negative neurons' cilia generally point in the SO direction. The white boxes are enlarged. Cilia basal body is bigger than axoneme, allowing for determining cilia orientation. **(*H-I*)** Allen Brain Atlas *in situ* hybridization staining of Col11a1 and Htr1a in mouse hippocampal CA1 at P56. Col11a1 is mostly expressed in the deep sublayer, but also slightly dispersed to the superficial sublayer ***(H)***. Htr1a is mostly present in the superficial sublayer and covers most, but not all area of SP ***(I)***. Images credit: Allen Institute for Brain Science. Super: superficial sublayer; Deep, deep sublayer. P7: Postnatal Day 7. SP: stratum pyramidale; SO: stratum oriens; SR: stratum radiatum. Images credit: Allen Institute for Brain Science

Fig. 2. Strong regulation of CA1 neuronal cilia length by Arl13B. ***(A-B)*** Transgenic Arl13B mice (Arl13B+) have much longer neuronal primary cilia than WT mice in the hippocampal subregions (CA1, CA3 and DG) in adults. Notably, CA1 region has the longest primary cilia and the effect of Arl13B on promoting cilia length is very strong. Compared with WT mice, the average CA1 cilia length increases by over 60% in Arl13B+ mice. ***(C-D)*** Primary cilia length is not strongly changed in other brain regions such as cortex and amygdale. Immunostaining of neuronal primary cilia in WT controls and Arl13B

overexpression transgenic (Arl13B+) mice. Unpaired Student's T-test, ***, $p < 0.001$; N.S., not significant. Scale bar: 10 µm. Data were collected from at least 3 young adult mice for each genotype. Mix sex.

Fig. 3. Opposite primary cilia orientation and marked cilia orientation changes in the hippocampal SP of Arl13B+ mice. ***(A-C)*** Deep- and superficial-sublayer neurons in ARl13B+ mice display opposite primary cilia orientation. ***(A)*** Postnatal cilia orientation changes at P7, P10, P14, P40, and P75. White boxes are enlarged at the bottom. White arrows indicate the mother centriole or the base of cilium, yellow arrows denote some centrin2-GFP artifacts. After P14, green artifacts caused by Centrin2-GFP expression became prominent (66, 71), but Centrin2-GFP was still able to indicate the base of primary cilia. Scale bars: 10 µm. ***(B)*** Polar plots and histogram plots of cilia orientation of Arl13B+ mice. Cilia orientation is opposite, and the majority of primary cilia point to SR (to the south). ***(C)*** Comparison of the percentage of north-oriented cilia at different ages of Arl13B+ mice. Each triangle represents the percentage of north-oriented cilia from an area of CA1 SP for quantifying cilia orientation. The percentage of north-oriented cilia decreases significantly from P7, P10, to P14, and reaches a plateau after P14. N.S., not significant, ***P < 0.001, One-way ANOVA. ***(D)*** Comparison of north-oriented cilia percentage between Arl13B+ and Control mice (Centrin2-GFP single transgenic mice) at different ages. Arl13B+ mice have more north-oriented primary cilia in CA1 SP than Control mice at P7, at P14 and P40. Note that at P7 Control mice have not protruded primary cilia (Fig. 1). ***(E-F)*** The thickness of CA1 SP lamina in Arl13B+ mice decreases with age postnatally. ***P < 0.001, One-way ANOVA. Primary cilia of Arl13B+ mice are well aligned with radial axis at P14 (F). ***(G-H)*** Immunofluorescence staining using AC3 and calbindin antibodies on hippocampal slices from Arl13B+ mice and Control mice. Scale bars: 10 µm. (G) Primary cilia of calbindin-positive neurons mostly point in the direction of SR (white arrows), while those of calbindin-negative neurons generally point to SO (yellow arrows). ***(H)*** Statistical data of Arl13B+ and Control mice. Over 80% cilia in the calbindin-positive region (superficial sublayer) point in the SR direction and less than 30% cilia in the calbindin-negative region (deep sublayer) point in the SR direction ***P < 0.001, One-way ANOVA. SP: stratum pyramidale; SO: stratum oriens; SR: stratum radiatum. n = 3 mice, 3 regions in the CA1 of each mouse were selected for quantification. Exception: for P14 and P40 of Control mice, n = 2. Mix sex.

Fig. 4. Early-born pyramidal neurons protrude primary cilia and mature earlier than late-born neurons. ***(A)*** Left: WT mice do not express many hair-like primary cilia until P9. At P7, AC3 immunostaining signal is only detected at centrosomes (94), with limited enrichment at SP bottom. At P9,

primary cilia are expressed but very short. At P10, primary cilia show opposite orientation in SP, and most cilia in superficial sublayer point in the direction of SR (Fig. 1B). Right: Earlier expression of primary cilia in Arl13B+ mice. Arl13B+ mice at P3 start to protrude primary cilia and at P5 more cilia emerge, which are mostly from early-born neurons and pointed to SO. At P7, both early-born neurons and late-born neurons express primary cilia. Cilia of early-born neurons point to SO, whereas cilia of late-born neurons point to SR. Many centrioles/cilia are highly condensed at SP bottom. Centrioles were marked by Centrin2-GFP. Data were collected from at least 3 mice each group. Scale bars: 10 µm. ***(B)*** Primary cilia first emerge from deep-sublayer neurons, then from superficial-sublayer neurons. Primary cilia length of deep- and superficial-sublayer neurons of Arl13B+ mice at P3, P7, P10, and P14. At P14, cilia length reaches the steady-state and cilia length has no difference between two sublayers. Over 280 total cilia were quantified in each subject. Unpaired Student's T-test, ***, $p < 0.001$; N.S., not significant. ***(C)*** NeuN expression was first detected in deep-layer CA1 neurons at P1, more at P5, then extended to superficial-layer neurons P7. At P14, both deep- and superficial-layer neurons had abundant NeuN expression. Scale bars: 10 µm***. (D-E)*** Allen Brain Atlas in situ hybridization (ISH) results of Shank3 and Homer1, two synaptic makers of excitatory neurons, in hippocampal CA1 at P4 and P14. At P4, Shank3 and Homer1 are only expressed in deep sublayer in hippocampal SP and Layer V (deep sublayer) of the neocortex. At P14, ISH signals of two genes occupy most area of SP and the six layers in the neocortex. Scale bars: 100 µm. Super: superficial sublayer; Deep, deep sublayer. (F) The hippocampal CA3 region of WT mice abundantly express primary cilia at P7, earlier than the CA1. Scale bars: 10 µm. (G) CA3 pyramidal neurons mature earlier than CA1 neurons. At P4, CamK2a and PSD-95, two postsynaptic marker proteins, are highly and widely expressed in CA3. In contrast, their expression are only restricted to the deep sublayer of CA1, not present in the superficial sublayer at P4. Scale bars: 100 µm. ISH images were adopted from the Allen Brain Atlas Developing Mouse Brain. Images credit: Allen Institute for Brain Science.

Fig. 5. Centriole/cilia of late-born neurons undergo a reverse movement after being clustered at SP bottom. ***(A-D)*** Centrioles are clustered at SP bottom from P3 to P7 and then re-distribute back to main SP. ***(A)*** Both Arl13B+ mice (Arl13B-mCherry;Centrin2-GFP mice) and Control mice (Centrin2-GFP littermates) showed a clustering pattern of centrioles in SP bottom from P3 to P7, and then re-distributed back to main SP at P10. Scale bars: 10 µm. ***(B)*** Quantification of the number of nuclei per square millimeter (Nuclei/mm^2) in the middle and bottom panels of SP from P3 to P14. The middle and bottom panel of SP as well as SR are defined in ***(I)*** and Methods Section. B: bottom; M: middle. ***(C)*** Quantification

of centriole number per square millimeter (centrioles/mm^2) in the middle and bottom panel of SP from P3 to P14. B: bottom; M: middle. ***(D)*** The ratio of centriole to nucleus (C/N Ratio) at SP bottom and SR from P3 to P14. C/N Ratio data were collected from the bottom panel of SP in combination with SR panel (See ***I***). ***(E)*** Centriole/cilia of late-born neurons exhibit a reverse movement after being clustered at SP bottom. Centrioles/cilia had dramatic changes in orientation and length at SP bottom from P7 to P14. Enlarged cilia images of late-born neurons show that cilia length at the superficial sublayer of SP was increasing, and cilia and centrioles were migrating upward (from SR to SO) from P7 to P14. Centrioles (arrows) in the front were followed by cilia axoneme. The P7 image is from Figure 3A. Scale bars: 10 µm. ***(F)*** A schematic model depicting the reverse movement of centrioles/cilia of late-born neurons in the dorsal hippocampus for cell positioning. Late-born neurons move against the saltatory migration direction back to main SP. It is unclear if early-born neurons, with opposite cilia orientation, have forward movement during this period. ***(G)*** Polar plots of cilia orientation in the upper part of SP from P7 to P14. Upper part: 70% top part of SP. Primary cilia in the upper part of SP at P7 largely pointed in the direction of SO (to the north). However, from P7 to P14, many south-oriented primary cilia moved back to main SP, consequently changing the cilia orientation in the upper part of SP. ***(H)*** The percentage of south-oriented cilia in the upper part of SP significantly increases from P7 to P14, confirming that late-born neurons continuously moved back to occupy the main SP during that period. ***P < 0.001, One-way ANOVA. P: postnatal. Number: days. n = 3. We selected 3 CA1 regions each mouse for quantification. Mix sex. Exception: P14 Control, n = 2, mix sex. (*I*) An example showing how the middle and bottom panel of SP as well as SR were defined and used for quantification, and more details are found in the "Materials and Methods". Scale bars: 10 µm.

Fig. 6. Primary cilia in both superficial and deep sublayers of the neocortex point to the pial surface. ***(A-C)*** Cilia orientation pattern in Layer II/III (superficial sublayer) and Layer V (deep sublayer) in the neocortex. ***(A)*** Left, immunostaining results of the superficial sublayer and deep sublayer in the neocortex from P14 and P40 from Arl13B+ mice. Scale bars: 10 µm. Right: Cilia orientation was quantified and summarized by polar plots (method details for polar plots can be found in Fig. 1*B-C*). Most primary cilia perpendicularly pointed to the pial surface in both superficial and deep sublayers of the neocortex. ***(B)*** Statistical data showing that over 70% of cilia point to the north (the pial surface) in both superficial and deep sublayer in the neocortex, but superficial sublayer has higher percentage of north-oriented cilia than deep sublayer. N.S., not significant, ***P < 0.001, Two-way ANOVA. ***(C)*** A schematic of cilia orientation generally in sublayers of the neocortex. Data for cilia orientation in Layer VI were collected, but not

shown here. Layer I does not have many pyramidal neurons, and we have not examined neuronal cilia in Layer IV. n = 3. Each mouse provided 3 different cortical regions for cilia quantification. Mix sex.

Fig. 7. Late-born cortical pyramidal cells also exhibit a reverse movement before P14 and protrude cilia later than early-born neurons. ***(A-D)*** The densities of centrioles and nuclei in the superficial sublayer (Layer II/III) of the neocortex changed from compact and uneven at P3 to sparse and even at P14. Confocal images of Layer II/III at P3 and P14 of Arl13B+ mice ***(A)***. WT mice exhibited a similar distribution pattern (not shown). The top and middle panels (as depicted) of superficial sublayer (Layer II/III) are enlarged on the right. Scale bars: 10 µm. The density of centrioles ***(B)*** and nuclei ***(C)*** at top and middle panels. Note that the density of centrioles and nuclei at P3 are higher than those of P14, which could be in part due to an increase in brain and cell body volume with age. ***(D)*** The ratio of centriole to nucleus (C/N ratio). N.S., not significant. Two-way ANOVA. ***(E-H)*** Early-born cortical neurons express primary cilia earlier than late-born neurons. ***(E-G)*** Co-immunostaining of AC3, Arl13B and DAPI in Layer II and V on brain slices at P3 and P7 from WT mice **(*E*)** and Arl13B+ mice ***(G)***. Scale bars: 5 µm. ***(F, H)*** Quantification of cilia length in cortical Layer II and V. Primary cilia of early-born neurons are much longer than those of late-born neurons at P3 and P7 in both WT ***(F)*** and Arl13B+ mice ***(H)***. n = 3 mice for each group. Three different regions in the cortex each mouse were selected for cilia quantification. Mix sex.

References

1. Bishop, G. A., Berbari, N. F., Lewis, J., and Mykytyn, K. (2007) Type III adenylyl cyclase localizes to primary cilia throughout the adult mouse brain. *J Comp Neurol* **505**, 562-571
2. Sterpka, A., and Chen, X. (2018) Neuronal and astrocytic primary cilia in the mature brain. *Pharmacol Res* **137**, 114-121
3. Singla, V., and Reiter, J. F. (2006) The primary cilium as the cell's antenna: signaling at a sensory organelle. *Science* **313**, 629-633
4. Valente, E. M., Rosti, R. O., Gibbs, E., and Gleeson, J. G. (2014) Primary cilia in neurodevelopmental disorders. *Nat Rev Neurol* **10**, 27-36
5. Lee, J. E., and Gleeson, J. G. (2011) Cilia in the nervous system: linking cilia function and neurodevelopmental disorders. *Curr Opin Neurol* **24**, 98-105
6. Guemez-Gamboa, A., Coufal, N. G., and Gleeson, J. G. (2014) Primary cilia in the developing and mature brain. *Neuron* **82**, 511-521
7. Lee, J. H., and Gleeson, J. G. (2010) The role of primary cilia in neuronal function. *Neurobiol Dis* **38**, 167-172
8. Houlden, H., Johnson, J., Gardner-Thorpe, C., Lashley, T., Hernandez, D., Worth, P., Singleton, A. B., Hilton, D. A., Holton, J., Revesz, T., Davis, M. B., Giunti, P., and Wood, N. W. (2007) Mutations in TTBK2, encoding a kinase implicated in tau phosphorylation, segregate with spinocerebellar ataxia type 11. *Nat Genet* **39**, 1434-1436

9. Goetz, S. C., Liem, K. F., Jr., and Anderson, K. V. (2012) The spinocerebellar ataxia-associated gene Tau tubulin kinase 2 controls the initiation of ciliogenesis. *Cell* **151**, 847-858
10. Bowie, E., Norris, R., Anderson, K. V., and Goetz, S. C. (2018) Spinocerebellar ataxia type 11-associated alleles of Ttbk2 dominantly interfere with ciliogenesis and cilium stability. *PLoS Genet* **14**, e1007844
11. Ikeuchi, Y., de la Torre-Ubieta, L., Matsuda, T., Steen, H., Okazawa, H., and Bonni, A. (2013) The XLID protein PQBP1 and the GTPase Dynamin 2 define a signaling link that orchestrates ciliary morphogenesis in postmitotic neurons. *Cell Rep* **4**, 879-889
12. Hasenpusch-Theil, K., and Theil, T. (2021) The Multifaceted Roles of Primary Cilia in the Development of the Cerebral Cortex. *Front Cell Dev Biol* **9**, 630161
13. Park, S. M., Jang, H. J., and Lee, J. H. (2019) Roles of Primary Cilia in the Developing Brain. *Front Cell Neurosci* **13**, 218
14. Ruat, M., Roudaut, H., Ferent, J., and Traiffort, E. (2012) Hedgehog trafficking, cilia and brain functions. *Differentiation* **83**, S97-104
15. Bangs, F., and Anderson, K. V. (2017) Primary Cilia and Mammalian Hedgehog Signaling. *Cold Spring Harb Perspect Biol* **9**
16. Pal, K., and Mukhopadhyay, S. (2015) Primary cilium and sonic hedgehog signaling during neural tube patterning: role of GPCRs and second messengers. *Dev Neurobiol* **75**, 337-348
17. Mukhopadhyay, S., Wen, X., Ratti, N., Loktev, A., Rangell, L., Scales, S. J., and Jackson, P. K. (2013) The ciliary G-protein-coupled receptor Gpr161 negatively regulates the Sonic hedgehog pathway via cAMP signaling. *Cell* **152**, 210-223
18. Dessaud, E., McMahon, A. P., and Briscoe, J. (2008) Pattern formation in the vertebrate neural tube: a sonic hedgehog morphogen-regulated transcriptional network. *Development* **135**, 2489-2503
19. Gorivodsky, M., Mukhopadhyay, M., Wilsch-Braeuninger, M., Phillips, M., Teufel, A., Kim, C., Malik, N., Huttner, W., and Westphal, H. (2009) Intraflagellar transport protein 172 is essential for primary cilia formation and plays a vital role in patterning the mammalian brain. *Dev Biol* **325**, 24-32
20. Higginbotham, H., Guo, J., Yokota, Y., Umberger, N. L., Su, C. Y., Li, J., Verma, N., Hirt, J., Ghukasyan, V., Caspary, T., and Anton, E. S. (2013) Arl13b-regulated cilia activities are essential for polarized radial glial scaffold formation. *Nat Neurosci* **16**, 1000-1007
21. Wechsler-Reya, R. J., and Scott, M. P. (1999) Control of neuronal precursor proliferation in the cerebellum by Sonic Hedgehog. *Neuron* **22**, 103-114
22. Spassky, N., Han, Y. G., Aguilar, A., Strehl, L., Besse, L., Laclef, C., Ros, M. R., Garcia-Verdugo, J. M., and Alvarez-Buylla, A. (2008) Primary cilia are required for cerebellar development and Shh-dependent expansion of progenitor pool. *Dev Biol* **317**, 246-259
23. Chizhikov, V. V., Davenport, J., Zhang, Q., Shih, E. K., Cabello, O. A., Fuchs, J. L., Yoder, B. K., and Millen, K. J. (2007) Cilia proteins control cerebellar morphogenesis by promoting expansion of the granule progenitor pool. *J Neurosci* **27**, 9780-9789
24. Amador-Arjona, A., Elliott, J., Miller, A., Ginbey, A., Pazour, G. J., Enikolopov, G., Roberts, A. J., and Terskikh, A. V. (2011) Primary cilia regulate proliferation of amplifying progenitors in adult hippocampus: implications for learning and memory. *J Neurosci* **31**, 9933-9944
25. Breunig, J. J., Sarkisian, M. R., Arellano, J. I., Morozov, Y. M., Ayoub, A. E., Sojitra, S., Wang, B., Flavell, R. A., Rakic, P., and Town, T. (2008) Primary cilia regulate hippocampal neurogenesis by mediating sonic hedgehog signaling. *Proc Natl Acad Sci U S A* **105**, 13127-13132
26. Berbari, N. F., Malarkey, E. B., Yazdi, S. M., McNair, A. D., Kippe, J. M., Croyle, M. J., Kraft, T. W., and Yoder, B. K. (2014) Hippocampal and cortical primary cilia are required for aversive memory in mice. *PLoS One* **9**, e106576

27. Tsai, L. H., and Gleeson, J. G. (2005) Nucleokinesis in neuronal migration. *Neuron* **46**, 383-388
28. Pocha, S. M., and Montell, D. J. (2014) Cellular and molecular mechanisms of single and collective cell migrations in Drosophila: themes and variations. *Annu Rev Genet* **48**, 295-318
29. Hatten, M. E. (1999) Central nervous system neuronal migration. *Annu Rev Neurosci* **22**, 511-539
30. Marin, O., Valiente, M., Ge, X., and Tsai, L. H. (2010) Guiding neuronal cell migrations. *Cold Spring Harb Perspect Biol* **2**, a001834
31. Marin, O., and Rubenstein, J. L. (2003) Cell migration in the forebrain. *Annu Rev Neurosci* **26**, 441-483
32. Rahimi-Balaei, M., Bergen, H., Kong, J., and Marzban, H. (2018) Neuronal Migration During Development of the Cerebellum. *Front Cell Neurosci* **12**, 484
33. Kuijpers, M., and Hoogenraad, C. C. (2011) Centrosomes, microtubules and neuronal development. *Mol Cell Neurosci* **48**, 349-358
34. Higginbotham, H. R., and Gleeson, J. G. (2007) The centrosome in neuronal development. *Trends Neurosci* **30**, 276-283
35. Rivas, R. J., and Hatten, M. E. (1995) Motility and cytoskeletal organization of migrating cerebellar granule neurons. *J Neurosci* **15**, 981-989
36. Kawauchi, T. (2015) Cellullar insights into cerebral cortical development: focusing on the locomotion mode of neuronal migration. *Front Cell Neurosci* **9**, 394
37. Xie, Z., Sanada, K., Samuels, B. A., Shih, H., and Tsai, L. H. (2003) Serine 732 phosphorylation of FAK by Cdk5 is important for microtubule organization, nuclear movement, and neuronal migration. *Cell* **114**, 469-482
38. Satir, P., and Christensen, S. T. (2007) Overview of structure and function of mammalian cilia. *Annu Rev Physiol* **69**, 377-400
39. Ishikawa, T., Ueno, H., Omori, T., and Kikuchi, K. (2021) Cilia and centrosomes: Ultrastructural and mechanical perspectives. *Semin Cell Dev Biol* **110**, 61-69
40. Khayyeri, H., Barreto, S., and Lacroix, D. (2015) Primary cilia mechanics affects cell mechanosensation: A computational study. *J Theor Biol* **379**, 38-46
41. Bezares-Calderon, L. A., Berger, J., and Jekely, G. (2020) Diversity of cilia-based mechanosensory systems and their functions in marine animal behaviour. *Philos Trans R Soc Lond B Biol Sci* **375**, 20190376
42. Resnick, A., and Hopfer, U. (2007) Force-response considerations in ciliary mechanosensation. *Biophys J* **93**, 1380-1390
43. Prasad, R. M., Jin, X., and Nauli, S. M. (2014) Sensing a sensor: identifying the mechanosensory function of primary cilia. *Biosensors (Basel)* **4**, 47-62
44. Spasic, M., and Jacobs, C. R. (2017) Primary cilia: Cell and molecular mechanosensors directing whole tissue function. *Semin Cell Dev Biol* **71**, 42-52
45. Shinohara, K., Kawasumi, A., Takamatsu, A., Yoshiba, S., Botilde, Y., Motoyama, N., Reith, W., Durand, B., Shiratori, H., and Hamada, H. (2012) Two rotating cilia in the node cavity are sufficient to break left-right symmetry in the mouse embryo. *Nat Commun* **3**, 622
46. Matsumoto, M., Sawada, M., Garcia-Gonzalez, D., Herranz-Perez, V., Ogino, T., Bang Nguyen, H., Quynh Thai, T., Narita, K., Kumamoto, N., Ugawa, S., Saito, Y., Takeda, S., Kaneko, N., Khodosevich, K., Monyer, H., Garcia-Verdugo, J. M., Ohno, N., and Sawamoto, K. (2019) Dynamic Changes in Ultrastructure of the Primary Cilium in Migrating Neuroblasts in the Postnatal Brain. *J Neurosci* **39**, 9967-9988
47. Cembrowski, M. S., Bachman, J. L., Wang, L., Sugino, K., Shields, B. C., and Spruston, N. (2016) Spatial Gene-Expression Gradients Underlie Prominent Heterogeneity of CA1 Pyramidal Neurons. *Neuron* **89**, 351-368

48. Cembrowski, M. S., and Spruston, N. (2019) Heterogeneity within classical cell types is the rule: lessons from hippocampal pyramidal neurons. *Nat Rev Neurosci* **20**, 193-204
49. Soltesz, I., and Losonczy, A. (2018) CA1 pyramidal cell diversity enabling parallel information processing in the hippocampus. *Nat Neurosci* **21**, 484-493
50. Hayashi, K., Kubo, K., Kitazawa, A., and Nakajima, K. (2015) Cellular dynamics of neuronal migration in the hippocampus. *Front Neurosci* **9**, 135
51. Mizuseki, K., Diba, K., Pastalkova, E., and Buzsaki, G. (2011) Hippocampal CA1 pyramidal cells form functionally distinct sublayers. *Nat Neurosci* **14**, 1174-1181
52. Danielson, N. B., Zaremba, J. D., Kaifosh, P., Bowler, J., Ladow, M., and Losonczy, A. (2016) Sublayer-Specific Coding Dynamics during Spatial Navigation and Learning in Hippocampal Area CA1. *Neuron* **91**, 652-665
53. Khalaf-Nazzal, R., and Francis, F. (2013) Hippocampal development - old and new findings. *Neuroscience* **248**, 225-242
54. Deguchi, Y., Donato, F., Galimberti, I., Cabuy, E., and Caroni, P. (2011) Temporally matched subpopulations of selectively interconnected principal neurons in the hippocampus. *Nat Neurosci* **14**, 495-504
55. Cooper, J. A. (2008) A mechanism for inside-out lamination in the neocortex. *Trends Neurosci* **31**, 113-119
56. Reiner, O. (2013) LIS1 and DCX: Implications for Brain Development and Human Disease in Relation to Microtubules. *Scientifica (Cairo)* **2013**, 393975
57. Silva, C. G., Peyre, E., and Nguyen, L. (2019) Cell migration promotes dynamic cellular interactions to control cerebral cortex morphogenesis. *Nat Rev Neurosci* **20**, 318-329
58. Chen, X., Luo, J., Leng, Y., Yang, Y., Zweifel, L. S., Palmiter, R. D., and Storm, D. R. (2016) Ablation of Type III Adenylyl Cyclase in Mice Causes Reduced Neuronal Activity, Altered Sleep Pattern, and Depression-like Phenotypes. *Biol Psychiatry* **80**, 836-848
59. Qiu, L., LeBel, R. P., Storm, D. R., and Chen, X. (2016) Type 3 adenylyl cyclase: a key enzyme mediating the cAMP signaling in neuronal cilia. *Int J Physiol Pathophysiol Pharmacol* **8**, 95-108
60. Ferent, J., Constable, S., Gigante, E. D., Yam, P. T., Mariani, L. E., Legue, E., Liem, K. F., Jr., Caspary, T., and Charron, F. (2019) The Ciliary Protein Arl13b Functions Outside of the Primary Cilium in Shh-Mediated Axon Guidance. *Cell Rep* **29**, 3356-3366 e3353
61. Guo, J., Otis, J. M., Higginbotham, H., Monckton, C., Cheng, J., Asokan, A., Mykytyn, K., Caspary, T., Stuber, G. D., and Anton, E. S. (2017) Primary Cilia Signaling Shapes the Development of Interneuronal Connectivity. *Dev Cell* **42**, 286-300 e284
62. Higginbotham, H., Eom, T. Y., Mariani, L. E., Bachleda, A., Hirt, J., Gukassyan, V., Cusack, C. L., Lai, C., Caspary, T., and Anton, E. S. (2012) Arl13b in primary cilia regulates the migration and placement of interneurons in the developing cerebral cortex. *Dev Cell* **23**, 925-938
63. Li, Y., Tian, X., Ma, M., Jerman, S., Kong, S., Somlo, S., and Sun, Z. (2016) Deletion of ADP Ribosylation Factor-Like GTPase 13B Leads to Kidney Cysts. *J Am Soc Nephrol* **27**, 3628-3638
64. He, K., Ma, X., Xu, T., Li, Y., Hodge, A., Zhang, Q., Torline, J., Huang, Y., Zhao, J., Ling, K., and Hu, J. (2018) Axoneme polyglutamylation regulated by Joubert syndrome protein ARL13B controls ciliary targeting of signaling molecules. *Nat Commun* **9**, 3310
65. Revenkova, E., Liu, Q., Gusella, G. L., and Iomini, C. (2018) The Joubert syndrome protein ARL13B binds tubulin to maintain uniform distribution of proteins along the ciliary membrane. *J Cell Sci* **131**
66. Sterpka, A., Yang, J., Strobel, M., Zhou, Y., Pauplis, C., and Chen, X. (2020) Diverged morphology changes of astrocytic and neuronal primary cilia under reactive insults. *Mol Brain* **13**, 28

67. Gigante, E. D., Taylor, M. R., Ivanova, A. A., Kahn, R. A., and Caspary, T. (2020) ARL13B regulates Sonic hedgehog signaling from outside primary cilia. *Elife* **9**
68. Larkins, C. E., Aviles, G. D., East, M. P., Kahn, R. A., and Caspary, T. (2011) Arl13b regulates ciliogenesis and the dynamic localization of Shh signaling proteins. *Mol Biol Cell* **22**, 4694-4703
69. Romani, M., Micalizzi, A., and Valente, E. M. (2013) Joubert syndrome: congenital cerebellar ataxia with the molar tooth. *Lancet Neurol* **12**, 894-905
70. Bangs, F. K., Schrode, N., Hadjantonakis, A. K., and Anderson, K. V. (2015) Lineage specificity of primary cilia in the mouse embryo. *Nat Cell Biol* **17**, 113-122
71. Higginbotham, H., Bielas, S., Tanaka, T., and Gleeson, J. G. (2004) Transgenic mouse line with green-fluorescent protein-labeled Centrin 2 allows visualization of the centrosome in living cells. *Transgenic Res* **13**, 155-164
72. Seixas, C., Choi, S. Y., Polgar, N., Umberger, N. L., East, M. P., Zuo, X., Moreiras, H., Ghossoub, R., Benmerah, A., Kahn, R. A., Fogelgren, B., Caspary, T., Lipschutz, J. H., and Barral, D. C. (2016) Arl13b and the exocyst interact synergistically in ciliogenesis. *Mol Biol Cell* **27**, 308-320
73. Sipos, E., Komoly, S., and Acs, P. (2018) Quantitative Comparison of Primary Cilia Marker Expression and Length in the Mouse Brain. *J Mol Neurosci* **64**, 397-409
74. Ponnio, T., and Conneely, O. M. (2004) nor-1 regulates hippocampal axon guidance, pyramidal cell survival, and seizure susceptibility. *Mol Cell Biol* **24**, 9070-9078
75. Valero, M., Cid, E., Averkin, R. G., Aguilar, J., Sanchez-Aguilera, A., Viney, T. J., Gomez-Dominguez, D., Bellistri, E., and de la Prida, L. M. (2015) Determinants of different deep and superficial CA1 pyramidal cell dynamics during sharp-wave ripples. *Nat Neurosci* **18**, 1281-1290
76. Radic, T., Friess, L., Vijikumar, A., Jungenitz, T., Deller, T., and Schwarzacher, S. W. (2017) Differential Postnatal Expression of Neuronal Maturation Markers in the Dentate Gyrus of Mice and Rats. *Front Neuroanat* **11**, 104
77. Fiala, J. C., Feinberg, M., Popov, V., and Harris, K. M. (1998) Synaptogenesis via dendritic filopodia in developing hippocampal area CA1. *J Neurosci* **18**, 8900-8911
78. Lauri, S. E., Vesikansa, A., Segerstrale, M., Collingridge, G. L., Isaac, J. T., and Taira, T. (2006) Functional maturation of CA1 synapses involves activity-dependent loss of tonic kainate receptor-mediated inhibition of glutamate release. *Neuron* **50**, 415-429
79. Thakar, S., Wang, L., Yu, T., Ye, M., Onishi, K., Scott, J., Qi, J., Fernandes, C., Han, X., Yates, J. R., 3rd, Berg, D. K., and Zou, Y. (2017) Evidence for opposing roles of Celsr3 and Vangl2 in glutamatergic synapse formation. *Proc Natl Acad Sci U S A* **114**, E610-E618
80. Sarnat, H. B., Nochlin, D., and Born, D. E. (1998) Neuronal nuclear antigen (NeuN): a marker of neuronal maturation in early human fetal nervous system. *Brain Dev* **20**, 88-94
81. Gusel'nikova, V. V., and Korzhevskiy, D. E. (2015) NeuN As a Neuronal Nuclear Antigen and Neuron Differentiation Marker. *Acta Naturae* **7**, 42-47
82. Reiter, J. F., Blacque, O. E., and Leroux, M. R. (2012) The base of the cilium: roles for transition fibres and the transition zone in ciliary formation, maintenance and compartmentalization. *EMBO Rep* **13**, 608-618
83. Chen, H. Y., Kelley, R. A., Li, T., and Swaroop, A. (2021) Primary cilia biogenesis and associated retinal ciliopathies. *Semin Cell Dev Biol* **110**, 70-88
84. Kitazawa, A., Kubo, K., Hayashi, K., Matsunaga, Y., Ishii, K., and Nakajima, K. (2014) Hippocampal pyramidal neurons switch from a multipolar migration mode to a novel "climbing" migration mode during development. *J Neurosci* **34**, 1115-1126
85. Kirschen, G. W., Liu, H., Lang, T., Liang, X., Ge, S., and Xiong, Q. (2017) The radial organization of neuronal primary cilia is acutely disrupted by seizure and ischemic brain injury. *Front Biol (Beijing)* **12**, 124-138

86. Angevine, J. B., Jr. (1965) Time of neuron origin in the hippocampal region. An autoradiographic study in the mouse. *Exp Neurol Suppl*, Suppl 2:1-70
87. Caviness, V. S., Jr. (1973) Time of neuron origin in the hippocampus and dentate gyrus of normal and reeler mutant mice: an autoradiographic analysis. *J Comp Neurol* **151**, 113-120
88. Stanfield, B. B., and Cowan, W. M. (1979) The development of the hippocampus and dentate gyrus in normal and reeler mice. *J Comp Neurol* **185**, 423-459
89. Xie, Z., Ma, X., Ji, W., Zhou, G., Lu, Y., Xiang, Z., Wang, Y. X., Zhang, L., Hu, Y., Ding, Y. Q., and Zhang, W. J. (2010) Zbtb20 is essential for the specification of CA1 field identity in the developing hippocampus. *Proc Natl Acad Sci U S A* **107**, 6510-6515
90. Hsia, A. Y., Malenka, R. C., and Nicoll, R. A. (1998) Development of excitatory circuitry in the hippocampus. *J Neurophysiol* **79**, 2013-2024
91. Isaac, J. T., Nicoll, R. A., and Malenka, R. C. (1995) Evidence for silent synapses: implications for the expression of LTP. *Neuron* **15**, 427-434
92. Xiao, M. Y., Wasling, P., Hanse, E., and Gustafsson, B. (2004) Creation of AMPA-silent synapses in the neonatal hippocampus. *Nat Neurosci* **7**, 236-243
93. Ball, G., and Seal, M. L. (2019) Individual variation in longitudinal postnatal development of the primate brain. *Brain Struct Funct* **224**, 1185-1201
94. Stoufflet, J., Chaulet, M., Doulazmi, M., Fouquet, C., Dubacq, C., Metin, C., Schneider-Maunoury, S., Trembleau, A., Vincent, P., and Caille, I. (2020) Primary cilium-dependent cAMP/PKA signaling at the centrosome regulates neuronal migration. *Sci Adv* **6**
95. Carvajal-Gonzalez, J. M., Roman, A. C., and Mlodzik, M. (2016) Positioning of centrioles is a conserved readout of Frizzled planar cell polarity signalling. *Nat Commun* **7**, 11135
96. Chien, Y. H., Srinivasan, S., Keller, R., and Kintner, C. (2018) Mechanical Strain Determines Cilia Length, Motility, and Planar Position in the Left-Right Organizer. *Dev Cell* **45**, 316-330 e314
97. Chen, X., Xia, Z., and Storm, D. R. (2012) Stimulation of electro-olfactogram responses in the main olfactory epithelia by airflow depends on the type 3 adenylyl cyclase. *J Neurosci* **32**, 15769-15778

Fig. 1

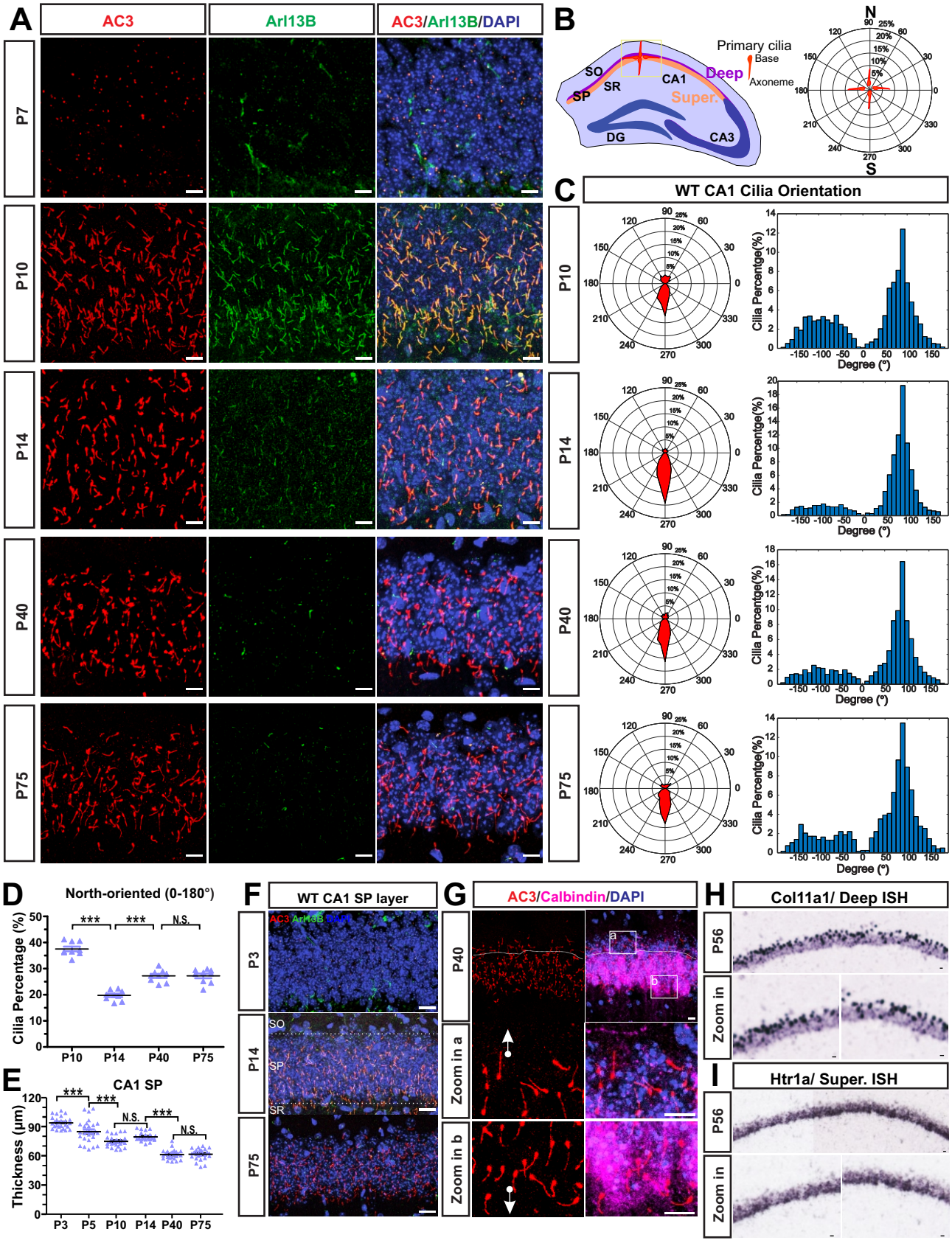
A
AC3
Arl13B
AC3/Arl13B/DAPI
P7
P10
P14
P40
P75
B
SO
SR
SP
CA1
Deep
Super.
DG
CA3
Primary cilia
Base
Axoneme
N
S
C
WT CA1 Cilia Orientation
Cilia Percentge(%)
Degree (°)
D
North-oriented (0-180°)
Cilia Percentage (%)
***
N.S.
P10
P14
P40
P75
E
CA1 SP
Thickness (μm)
P3
P5
F
WT CA1 SP layer
AC3 Arl13B DAPI
G
AC3/Calbindin/DAPI
Zoom in a
Zoom in b
H
Col11a1/ Deep ISH
Zoom in
I
Htr1a/ Super. ISH

Fig. 2

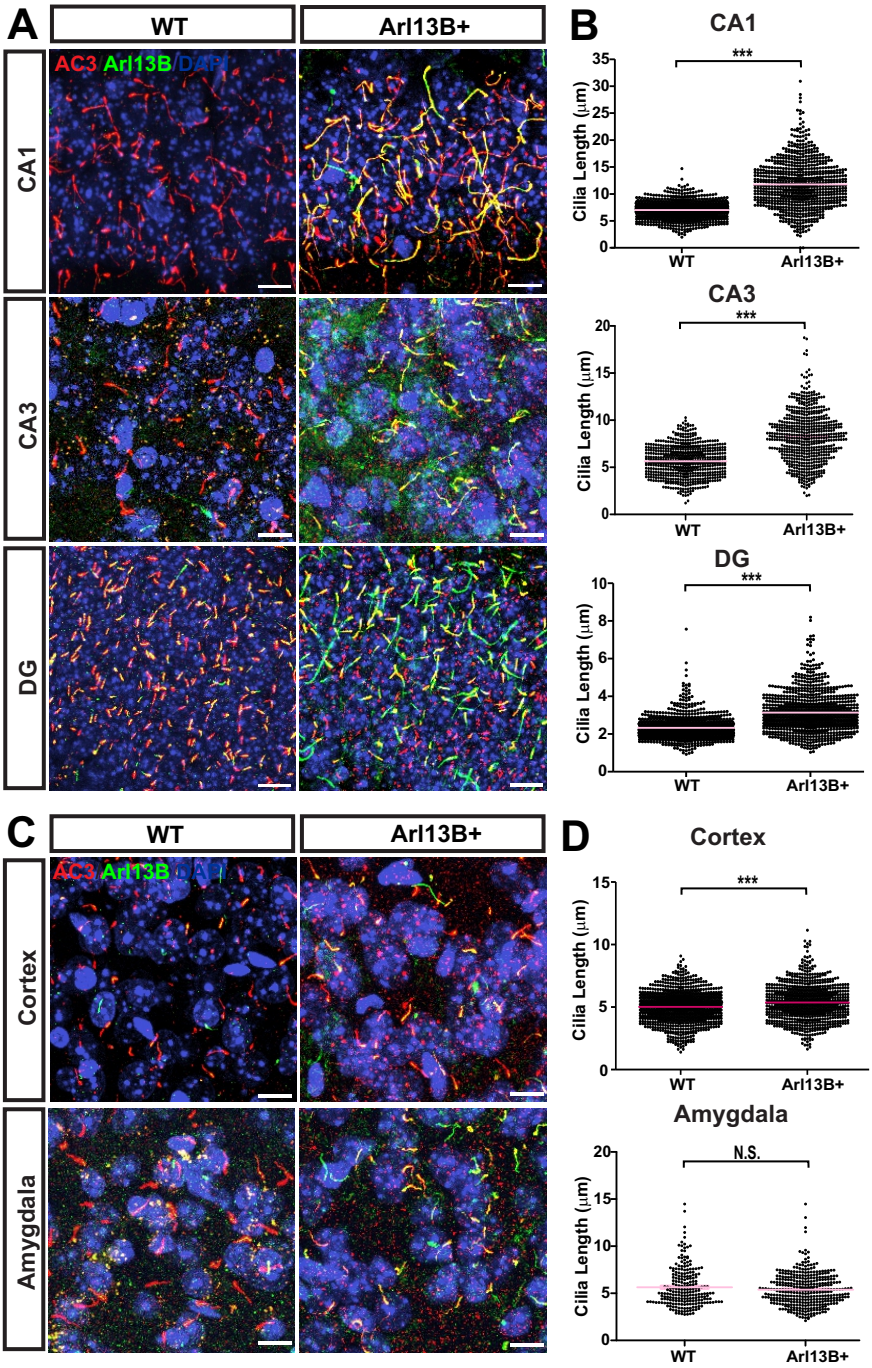
A
WT
Arl13B+
AC3/Arl13B/DAPI
CA1
CA3
DG
B
CA1
CA3
DG
***
Cilia Length (μm)
WT
Arl13B+
C
AC3/Arl13B/DAPI
Cortex
Amygdala
D
Cortex
Amygdala
N.S.

Fig. 3

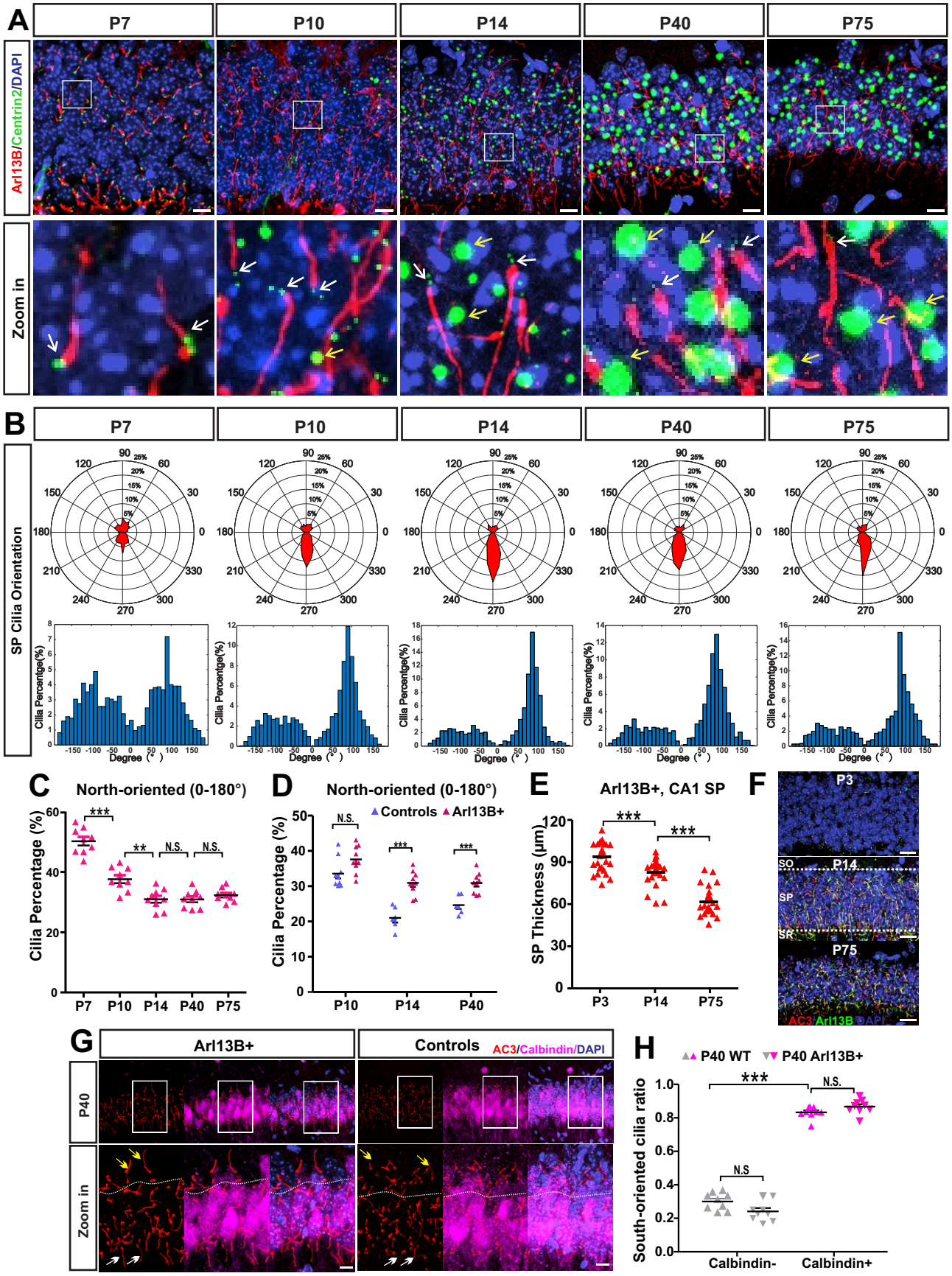
A
P7
P10
P14
P40
P75
Arl13B/Centrin2/DAPI
Zoom in
B
SP Cilia Orientation
Cilia Percentge(%)
Degree (°)
C
North-oriented (0-180°)
Cilia Percentage (%)
***
**
N.S.
N.S.
D
North-oriented (0-180°)
Controls
Arl13B+
Cilia Percentage (%)
N.S.
***
***
E
Arl13B+, CA1 SP
SP Thickness (μm)
***
***
F
P3
P14
P75
SO
SP
SR
AC3/Arl13B/DAPI
G
Arl13B+
Controls
AC3/Calbindin/DAPI
P40
Zoom in
H
P40 WT
P40 Arl13B+
South-oriented cilia ratio
***
N.S.
N.S
Calbindin-
Calbindin+

Fig. 4

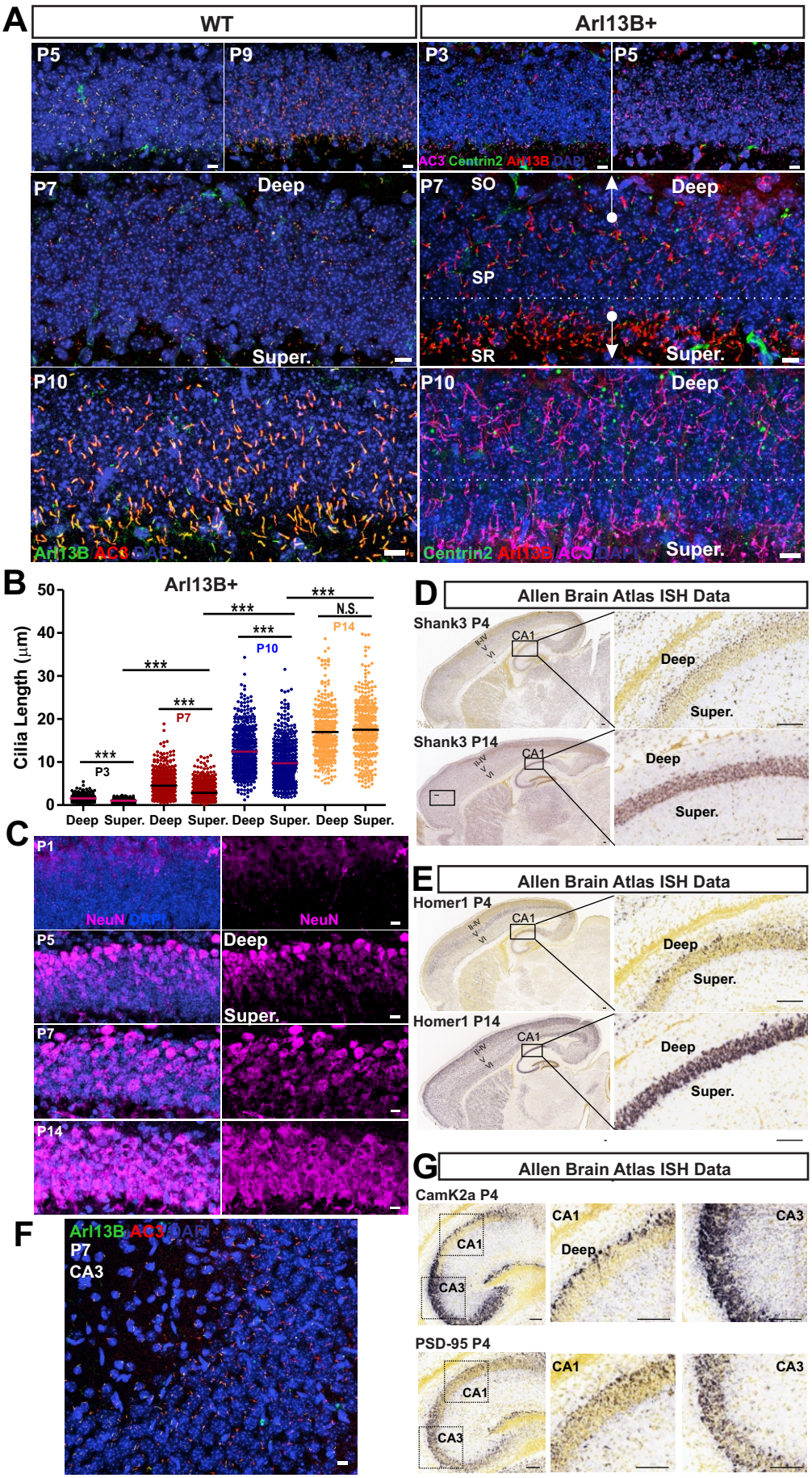
A
WT
Arl13B+
P5
P9
P3
P5
AC3 Centrin2 Arl13B DAPI
P7
Deep
Super.
P7
SO
Deep
SP
SR
Super.
P10
P10
Deep
Arl13B AC3 DAPI
Centrin2 Arl13B AC3 DAPI
Super.
B
Arl13B+
Cilia Length (μm)
50
40
30
20
10
0
***
P3
***
P7
***
***
P10
***
N.S.
P14
Deep Super. Deep Super. Deep Super. Deep Super.
C
P1
NeuN DAPI
NeuN
P5
Deep
Super.
P7
P14
D
Allen Brain Atlas ISH Data
Shank3 P4
CA1
Deep
Super.
Shank3 P14
CA1
Deep
Super.
E
Allen Brain Atlas ISH Data
Homer1 P4
CA1
Deep
Super.
Homer1 P14
CA1
Deep
Super.
F
Arl13B AC3 DAPI
P7
CA3
G
Allen Brain Atlas ISH Data
CamK2a P4
CA1
CA3
CA1
Deep
CA3
PSD-95 P4
CA1
CA3
CA1
CA3

Fig. 5

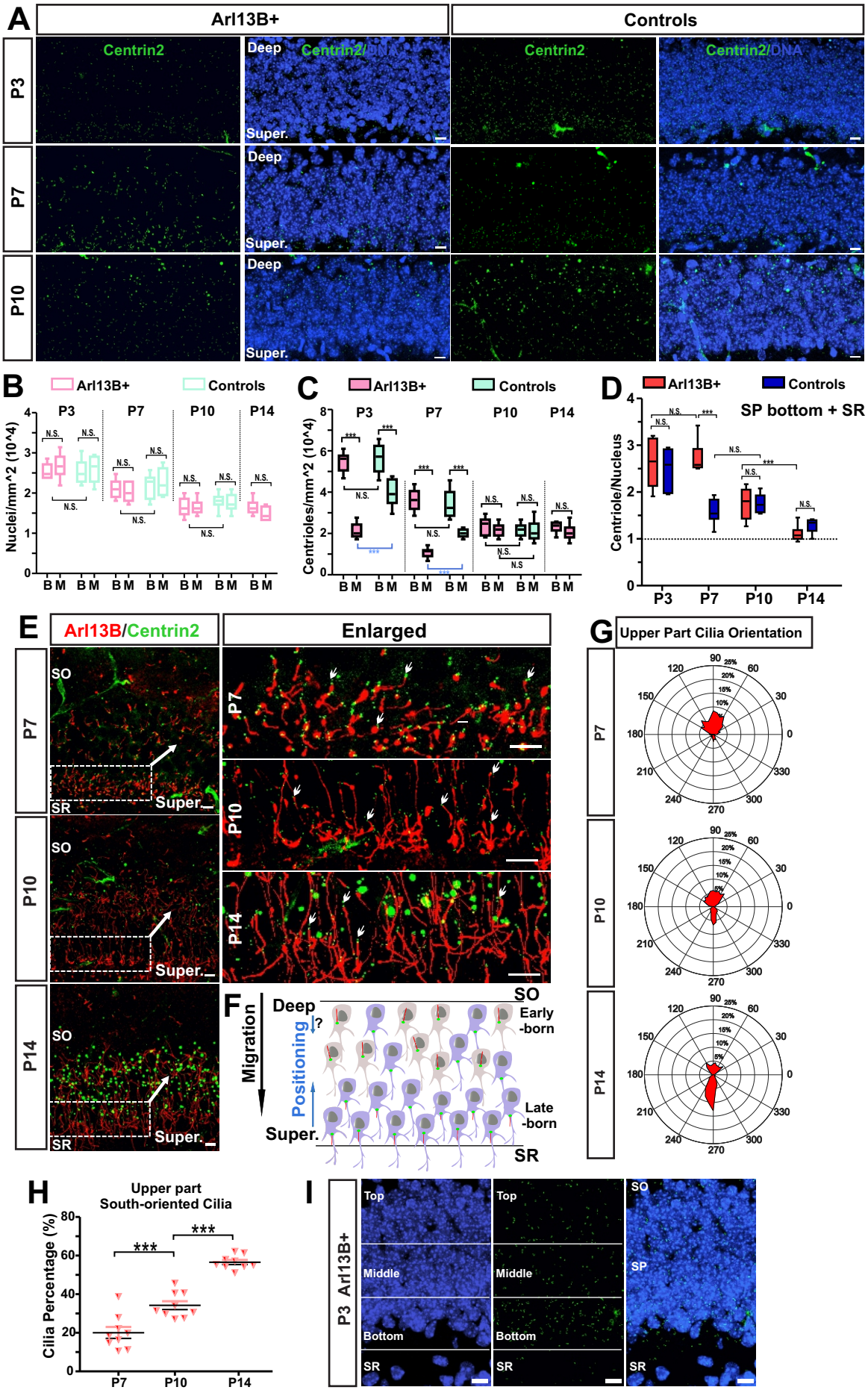
A
Arl13B+
Controls
P3
P7
P10
Centrin2
Centrin2/DNA
Deep
Super.
B
Arl13B+
Controls
P3
P7
P10
P14
Nuclei/mm^2 (10^4)
N.S.
B M
C
Centrioles/mm^2 (10^4)
***
D
SP bottom + SR
Centriole/Nucleus
E
Arl13B/Centrin2
Enlarged
SO
SR
Super.
F
Migration
Positioning
Deep
Super.
Early -born
Late -born
G
Upper Part Cilia Orientation
H
Upper part South-oriented Cilia
Cilia Percentage (%)
I
Top
Middle
Bottom
SP

Fig. 6

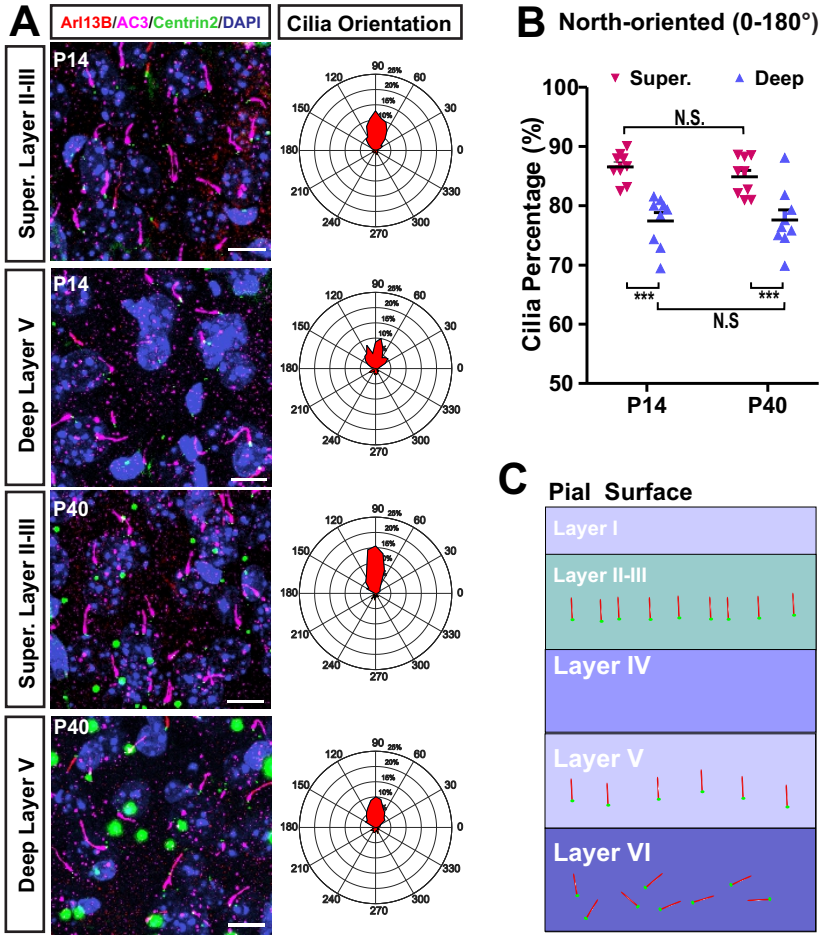
A
Arl13B/AC3/Centrin2/DAPI
Cilia Orientation
Super. Layer II-III
Deep Layer V
Super. Layer II-III
Deep Layer V
P14
P14
P40
P40
B
North-oriented (0-180°)
Super.
Deep
Cilia Percentage (%)
N.S.
***
N.S
***
P14
P40
C
Pial Surface
Layer I
Layer II-III
Layer IV
Layer V
Layer VI

Fig. 7

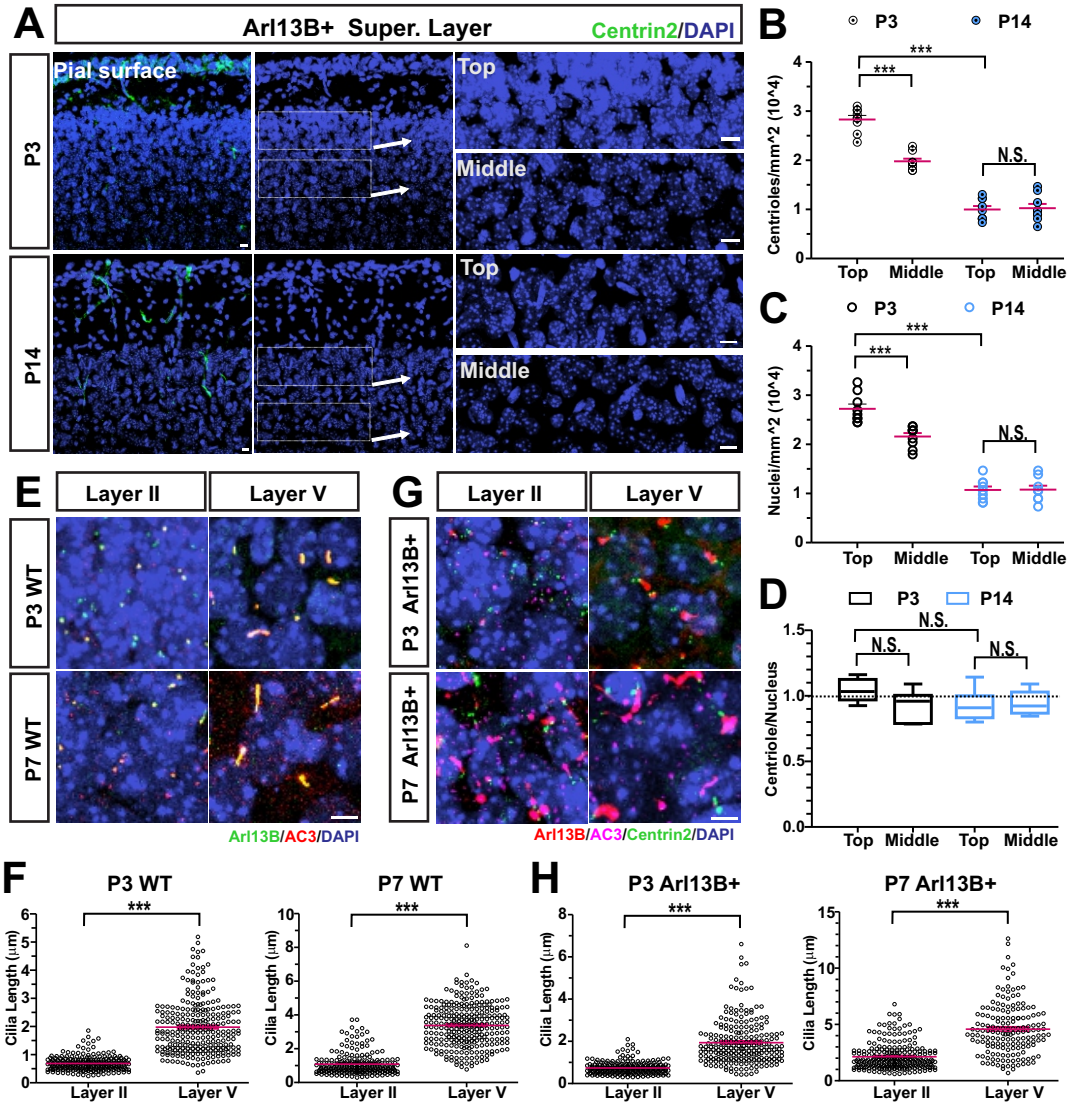
A
Arl13B+ Super. Layer
Centrin2/DAPI
P3
P14
Pial surface
Top
Middle
B
P3
P14
Centrioles/mm^2 (10^4)
***
N.S.
Top
Middle
C
Nuclei/mm^2 (10^4)
D
Centriole/Nucleus
E
Layer II
Layer V
P3 WT
P7 WT
Arl13B/AC3/DAPI
G
P3 Arl13B+
P7 Arl13B+
Arl13B/AC3/Centrin2/DAPI
F
P3 WT
P7 WT
Cilia Length (μm)
H
P3 Arl13B+
P7 Arl13B+